https://doi.org/10.5194/tc-2020-277
Preprint. Discussion started: 23 October 2020

The Cryosphere Discussions

Tree canopy and snow depth relationships at fine scales with terrestrial laser scanning

Ahmad Hojatimalekshah[1], Zach Uhlmann[1], Nancy F. Glenn[1], Christopher A. Hiemstra[2], Christopher J. Tennant[3], Jake D. Graham[1], Lucas Spaete[4], Art Gelvin[2], Hans-Peter Marshall[1], James McNamara[1], Josh Enterkine[1]

[1]Department of Geosciences, Boise State University, Boise, 83725, USA
[2]Cold Regions Research and Engineering Laboratory, Fort Wainwright, 99703, USA
[3]US Army Corps of Engineers, Sacramento, CA, 95814, USA
[4]Minnesota Department of Natural Resources, Division of Forestry, Resource Assessment, Grand Rapids, 55744, USA

Correspondence to: Nancy F. Glenn (nancyglenn@boisestate.edu)

Abstract. Understanding the impact of tree structure on snow depth and extent is important in order to make predictions of snow amounts, and how changes in forest cover may affect future water resources. In this work, we investigate snow depth under tree canopies and in open areas to quantify the role of tree structure in controlling snow depth, as well as the controls from wind and topography. We use fine scale terrestrial laser scanning (TLS) data collected across Grand Mesa, Colorado, USA, to measure the snow depth and extract horizontal and vertical tree descriptors (metrics) at six sites. We apply the Marker-controlled watershed algorithm for individual tree segmentation and measure the snow depth using the Multi-scale Model to Model Cloud Comparison algorithm. Canopy, topography and snow interaction results indicate that vegetation structural metrics (specifically foliage height diversity) along with local scale processes such as wind are highly influential on snow depth variation. Our study specifies that windward slopes show greater impact on snow accumulation than vegetation metrics. In addition, the results emphasize the importance of tree species and distribution on snow depth patterns. Fine scale analysis from TLS provides information on local scale controls, and provides an opportunity to be readily coupled with airborne or spaceborne lidar to investigate larger-scale controls on snow depth.

1 Introduction

Forests cover approximately half of the snow-covered landmasses on Earth during peak snow extent (Kim et al., 2017), with snow in nonpolar, cold climate zones accounting for 17 % of the total terrestrial water storage (Rutter et al., 2009; Guntner et al., 2007). Estimating the amount of water stored in this snowpack, the snow water equivalent (SWE), and its spatial distribution under various physiographic conditions, are crucial to providing water managers with parameters to accurately predict runoff timing, duration and amount, especially in a changing climate. Snowbound forested regions are rapidly changing in forest cover composition (e.g. fire, insect outbreaks, thinning) (Nolin and Daly, 2006; Bewley et al., 2010; Gauthier et al.,

https://doi.org/10.5194/tc-2020-277
Preprint. Discussion started: 23 October 2020

2015). Understanding how forest characteristics affects snow distribution, as well as how we might model the relationships between forests and snow distribution will benefit water management objectives.

Forest canopy cover can be incorporated into watershed and regional scale models as subgrid parameterization via snow depletion curves by relating canopy cover distributions to fractional melt patterns (Dickerson-Lange, et al., 2015; Homan et al., 2011; Luce et al., 1999). Pixel-level binary or weighted snow depth correction factors in gridded models (Hedrick et al., 2018, Winstral et al., 2013) can be adjusted for canopy cover, as well as a hybridized approach that adjusts radiative inputs differently in open areas and forest gaps based on their size and relationship to the surrounding forest (Seyednasrollah and Kumar, 2014). In research pertaining to forest-snow processes, forest plots may be classified qualitatively (e.g., Dickerson-Lange et al., 2015; Pomeroy et al., 2009) or more recently, at larger scales, quantitatively with airborne lidar (e.g. Mazzotti et al., 2019). The use of lidar in spatially distributed modeling efforts is rapidly advancing (e.g. Hedrick et al., 2018, Painter et al., 2016) and understanding how best to describe forest characteristics (cover, structure, gaps, etc.) relevant to snow distribution is evolving.

Airborne lidar has been used to describe snow depths in forests starting almost two decades ago (e.g. Hopkinson et al., 2004), and more recently, to describe the relationships among forest characteristics and snow distributions (e.g. Moeser et al., 2015a,b; Mazzotti et al., 2019; Zheng et al., 2016; Tennant et al., 2017). Realizing airborne lidar's capabilities to provide high-resolution snow depth and canopy measurements across large extents, studies have identified vegetation characteristics as drivers of snow depth variation. Canopy structure along with the forest canopy edge were driving factors that govern the snow depth distribution in a study of alpine climates (Mazzotti et al., 2019). Similarly, mean distance to canopy and canopy closure have been identified as strong metrics for predicting snow interception (Moeser et al., 2015a). Broxton et al. (2015) found canopy-snow interception and shading properties in transition zones result in different snow depths in comparison to the open and under-the-canopy regions. Further work in snow depth variability near forest edges acknowledges that snow depth variations are due to the effects of temperature, wind speed and direction, solar radiation, and forest distribution (Currier and Lundquist, 2018).

Terrestrial laser scanning (TLS) can provide fine-scale (plot-level) observations between forest cover and snow distribution that can be used to validate airborne lidar (e.g. Currier et al., 2019) and confidently upscale local-scale processes (Revuelto et al., 2016a,b). While many TLS studies have used the data to validate snow depths and melt (e.g. Deems et al., 2013; Hartzell et al., 2015; Grünewald et al., 2010), only a few studies have used TLS to further explore forest canopy – snow relationships (e.g. Revuelto et al., 2015, 2016a, b; Gleason et al., 2013). Revuelto et al. (2015, 2016b) found smaller snow depth differences between the canopy and open areas in regions of thicker snowpacks using TLS. They also demonstrated that the proximity to the trunk affects the snow depth distribution from shallower snow close to the trunks to deeper snow at the edge of the canopy. Gleason et al. (2013) used TLS to map tree stem density in burned forests and related this to greater snow accumulation in comparison to unburned areas.

Schirmer et al. (2011) investigated the topography and wind control on snow distribution patterns using multiple TLS snow depth collections, and observed the high contribution of storms in defining the snow accumulation pattern. They found that

https://doi.org/10.5194/tc-2020-277
Preprint. Discussion started: 23 October 2020

when canopy interception is dominant and wind effect is minimal, the variation in snow depth is controlled by vegetation characteristics. In the wind dominant case, Trujillo et al. (2007) observed that snow depth variability occurs at larger scales than those related to vegetation. These studies stress the importance of choosing proper scales to study the controlling processes on snow depth variability.

The objective of this study is to further contribute to the understanding of fine-scale forest canopy – snow interactions by exploring how forest canopy structure affects snow depth distribution during the snow accumulation period with TLS. This study is part of the NASA-led SnowEx 2017 campaign aimed at evaluating remote sensing snow properties with a primary focus on testing the impact of forest on remote sensing approaches for monitoring SWE. We use TLS data collected during the accumulation period in mid-winter SnowEx 2017 (winter 2016-2017) across a number of small TLS study sites on Grand Mesa, CO. In this study, we explore the following questions:

1. What measures of vegetation best describe a relationship with snow depth under the canopy (sub-canopy)?
2. Are there conditions in which vegetation characteristics are a more important control on snow depth than topography, or vice versa?
3. Does snow depth vary as a function of distance from the canopy edge? How does tree height influence snow depth as a function of distance and direction?

2 Method

2.1 Study Area

The TLS data were collected at six sites (A, F, K, M, N, and O) across Grand Mesa, Colorado, USA. Grand Mesa is an approximate 470 km^2 plateau with elevation of 2,922 to 3,440 m, rising along a west to east gradient (Fig. 1). Vegetation in the west, where wind speeds are highest, is predominantly shrubby cinquefoil (Dasiphorafruticosa) steppe with isolated Engelmann spruce (Piceaengelmannii) tree islands. The central portion of the mesa becomes semi-continuous forest cover consisting primarily of Engelmann spruce with minor subalpine fir (Abieslasiocarpa) and aspen (Populustremuloides) trees, all interspersed with subalpine meadows. Farther to the east, where wind speeds are lowest and elevation drops, there is dense continuous Engelmann spruce and subalpine fir forest with some lodgepole pine (Pinus contorta var. latifolia) and aspen stands at the lowest elevations.

Wind speed data during our TLS data collection period were available from three stations including a site at the western extent of forest cover on the plateau (Mesa West, near site A), a site termed the Local Scale Observation Site (LSOS), and a site situated in more dense forest in the middle of Grand Mesa (Mesa Middle, near site M) (Houser, personal comm.) (Fig. 2). The data were collected from 17 November 2016 – 28 February 2017 and indicate a dominant NE wind direction at site A, though up to 15 m/s wind speeds from the SW were observed at this site. The predominant wind direction was from the NW at LSOS, and from the NW and SE at site M, during the sampling period. In analyses outlined below, we utilized a general E-W direction for testing the importance of wind (whereas we used a N-S direction for testing shading effects on snow, more below).

https://doi.org/10.5194/tc-2020-277
Preprint. Discussion started: 23 October 2020

2.2 Terrestrial Laser Scanning

We collected TLS data in snow-off (fall 2016) and snow-on (winter 2017) conditions at Grand Mesa at several sites (Fig. 1, Table 1) (Glenn et al., 2019; Hiemstra et al., 2019). The winter 2017 data collection occurred over 16 days but without significant snowfall between days. Each site was scanned once during the duration. A Riegl VZ-1000 (1550 nm) and Leica Scan Station C10 (532 nm) were used. Multiple scans were obtained at each site and coregistered to produce a single point cloud for each site and date. Coregistered scans were then georegistered using surveyed locations within the plots. The georegistered scans (i.e. area of analysis) for each site ranges from approximately 10,000 to 38,000 m^2 (Table 1).

The TLS data were then utilized to derive snow depths, vegetation metrics, and topographic indices. From these data, we developed a series of statistical analyses to investigate relationships between the canopy and snow depths under the canopy at each of our sites. We also describe snow depths in open areas with no trees (of a least 0.5 m height). Methods on identifying individual trees, under the canopy and in the open, are described below.

2.3 TLS Data Processing

We processed the TLS data into returns from ground and vegetation (fall 2016) or snow and vegetation (winter 2017), and estimated snow depths at each of the sites, using several sub-routines in CloudCompare (v2.11 alpha; retrieved from http://www.cloudcompare.org/). We also used the TLS data to perform individual tree segmentation and extract vegetation parameters using R 3.5.3 (R Core Team, 2019), lidR (v3.1.1; Roussel) and rLiDAR (v0.1.1; Silva) packages. These steps are outlined in Fig. 3.

2.3.1 Ground, snow, and vegetation classification

We used the CANUPO method in CloudCompare to separate vegetation from ground and snow returns. This method includes training and classification. In the training step, we used 10,000 snow and vegetation samples to construct the classifier. We trained the algorithm at 15 different scales to assign features related to each class and selected the 9 best combinations of scales (0.1m, 0.2m, 0.25m, 0.5m, 0.75m, 1m, 2m, 3m, 5m) to properly separate different classes. The combination of information from these scales helped the algorithm detect the dimension of each feature and assign snow and vegetation labels to the unclassified point clouds (Lague et al., 2013). We found that CANUPO misclassified snow data points near tree stems as vegetation, and thus we reclassified these points manually using the software TerraScan (Helsinki, Finland).

2.3.2 Snow depth estimation

To estimate under-canopy and open-area snow depths, we used the M3C2 algorithm (Lague et al., 2013) in CloudCompare. In this algorithm, for every single point in the ground point cloud we defined a cylinder with a range of different radii (projection scales) varying from 10 cm to 3 m and a length (height) of 3 m (see Lague et al., 2013, for details on these parameters). The orientation of the cylinder was along the normal vector of planes fitted on the ground points within a 10cm radius. We projected

https://doi.org/10.5194/tc-2020-277
Preprint. Discussion started: 23 October 2020

all points within the cylinder onto the cylinder axis, took the vertical distance between projected snow, and ground points as the snow depth estimation. Through iteration, we found a balance between including enough TLS points for subsequent analysis and the accuracy of the snow depths by using a 1 m projection scale. Our resulting snow depth measurement has a relative accuracy of approximately 2.5 cm based on the maximum standard deviation from M3C2. Utilizing these measurements, we compared snow depths under the canopy and in the open at each site. We also defined a transition zone of 10 m from the canopy to the open to identify any relevant differences within this zone.

2.3.3 Individual tree segmentation and vegetation metrics

We developed a canopy height model at 0.5 m resolution and identified tree tops to segment individual trees in the R package lidR. We detected a local maxima to identify tree tops using window sizes ranging from 1-3 m and minimum tree heights from 2-6m, depending upon the site. For areas with lower tree heights (0.5 – 2m), we tiled the data that contained these trees and segmented them in a similar approach. This allowed us to more accurately segment distinctly shorter and taller tree populations within sites, by adjusting segmentation parameters that worked better for those areas. Based on our preliminary analyses, we found that the Marker-controlled watershed segmentation algorithm was most accurate (compared to li2012, dalponte2016, and watershed, all available in the lidR package). We found that in cases where tall and short trees are close to each other, the algorithm could not detect shorter trees with large crown radii, and if a small crown radii is used, the branches far from the top of the tree may be considered as an individual tree. We resolved this problem by tiling the las files and processing each separately and then combining the results. An example of the segmentation results from site F is shown in Fig. 4. A similar process was performed for all sites.

To define *under the canopy* and *in the open*, we first performed segmentation to identify individual trees. Under the canopy was defined by all snow depth points within the tree polygons. To define the open area, we merged individual tree polygons that were less than 3 m from each other (patches of trees) and used the remaining areas as open. Site A was the only site dominated by shrubs (Fig. 1, Table 1) and we considered the shrub area as open (we removed shrubs in the processing and kept the ground points below) at this site since the focus of our study was on tree-snow relationships.

We computed 22 vegetation metrics for each individual tree identified in the segmentation process (Tables 2, A1). We then used these metrics to predict snow depths at each site using a simple linear regression.

2.3.4 Influence of canopy edge on snow depth

We used the individual trees to predict snow depth at distances of 1 to 10 m away from the canopy edge. This represents how snow depth changes when we move from the edge of individual trees to the open within 10 m distance from the edge. We subsampled our data to only include trees that had good snow coverage (from TLS) under the canopy. This was determined based on an individual tree polygon containing a minimum of 10 snow pixels (pixel resolution of 0.5 m).

https://doi.org/10.5194/tc-2020-277
Preprint. Discussion started: 23 October 2020

2.3.5 Tree height

We investigated the correlation of maximum tree height (at the individual tree level) with snow depth as a function of distance from the canopy. We used 1 m distance bins and calculated the correlation between the maximum tree height and mean snow depth at each bin.

2.3.6 Topography

Slope and aspect were derived for each site using a nearest neighbor method at 1m grid resolution. We evaluated snow depth changes related to plot-scale (1 m) slope and aspect variations. We did this in both under the canopy and open areas at each site.

2.3.7 Gap distribution

We explored whether any of our sites were suitable for understanding the role of forest gaps (i.e. shading, interception) on snow depth distributions. While our study was not designed to analyze a range of gap distributions, the inherent forest density and distribution gradient that spanned our sites across Grand Mesa provided this opportunity. In particular, we sought to identify if sites had a dispersed tree pattern, such that the gaps were large enough to prevent canopy interception of snow, and thus accumulated deeper snow. Seyednasrollah and Kumar, (2014) used a relationship of tree height and gap radius for evaluation of net radiation. We derived a similar but simplified gap distribution approach (Equation 1). We calculated the average distance of 10 nearest trees to each individual tree. This gave us a rough estimate of a gap size around each tree (D). In the next step, we divided that average distance (D) by the average height (H) of those 10 nearest trees (D/H). This ultimately provides a ratio by which we can investigate the impact of shading from trees on gaps combined with gap size.

$$\frac{D_j}{H_j} = \frac{\frac{1}{k}\sum_{i=1}^{k} d_{ij}}{\frac{1}{k}\sum_{i=1}^{k} h_{ij}} \quad (1)$$

Equation (1), illustrates the gap distribution for an individual tree (j) where, D_j is the mean distance of the k closest trees to tree j; H_j is the average height of k closest trees to tree j; k is the number of neighbors and d_{ij} and h_{ij} are the distance and height of tree i to tree j, respectively.

Secondly, we performed an average nearest neighbor analysis of the distribution of trees at each of the sites. In this analysis, we tested for tightly clustered trees in which gaps were minimal (clustered), randomly distributed trees where gaps could potentially lead to deeper snow accumulation (random), or dispersed trees where no particular pattern exists and thus gaps are likely not prevalent (dispersed).

2.3.8 Directional analysis

We also investigated relationships between tree heights and snow depth based on direction. We did this using the 10 m transition zone (buffer) for each individual tree. We classified snow depths within each buffer in the four cardinal directions

https://doi.org/10.5194/tc-2020-277
Preprint. Discussion started: 23 October 2020

and computed the correlation between tree heights and mean snow depth per each direction. We compiled our tree height data with all tree heights analyzed together, as well as subsets of data with tree heights < 10 m and > 10 m. We also performed a directional analysis with a Wilcoxon signed-rank test for comparing snow depth on the north and south sides (and east and west) for individual trees at each site.

3 Results

3.1 Snow depths

Using our individual tree analysis, we found higher snow depths in open regions and lower snow depths in areas dominated with trees (see Table A2, Fig. B1). Snow depths were 12-28 % higher in the open than under canopy. Mean snow depth percent change between the 10m transition zone and under the canopy ranges from less than 1 % for sites A and K to a maximum of 7 % at site M. We found the lowest mean snow depths in our most westerly site (A), which is dominated by dense clusters of relatively rigid shrubs (Dasiphorafruticosa) and has the lowest tree cover of all sites. The standard deviation (SD) of snow depths was similar between the transition zone and under the canopy for four sites (A, F, K, and O). We found a significantly lower SD of open area snow depths at three of the sites (M, N, O) compared with under-canopy and transition zones (Table A2).

3.2 Influence of vegetation metrics on snow depth

Based on a linear regression, most sites had mid-to-high correlation between a specific vegetation metric (from Table 2) from individual trees and snow depths, with foliage height diversity (FHD), which was the most influential vegetation metric at four of the six sites (Tables 1, 3). Figure 5 shows the distribution of FHD at each of the sites, with higher FHD demonstrating more evenly spaced foliar arrangement along an individual tree. Most of the sites had two distributions of FHD. At sites F, K, N, O, the FHD and snow depth had negative correlations ranging from 0.35-0.75; as the foliar arrangement was more evenly spaced along an individual tree, snow depth decreased. At site A, a high negative correlation (0.68) between percentage of returns above 1 m (pzabov1) and snow depth occurred. FHD also had a relatively high negative correlation at this site (0.47) with snow depth.

3.3 Influence of slope and aspect on snow depth

We found that at site A, slope was influential on snow depths in the open. For example, slope explained 44 % of the variance of snow depth in the open at this site (Table 3). High snow depths were found in open northeast facing slopes (same as predominant wind direction) at site A (see Figs. 1, 6b). Site O was the only site that we found an influence of both slope and aspect, and this influence occurred in both the open and under the canopy (Table 3, Figs. 6a, b). This site has high north and west facing slopes (in both under canopy and the open) with relatively higher snow depths; whereas south facing slopes have relatively lower snow depths.

https://doi.org/10.5194/tc-2020-277
Preprint. Discussion started: 23 October 2020

215 **3.4 Influence of canopy edge on snow depth**

We found that snow depths increase with distance from the canopy edge into the open for the majority of individual trees (Fig. 7a). These correlations were typically above 0.60 and in many sites over 0.80. At some sites we found negative correlations between distance and snow depth (Fig. 7b and Figs. B2-7 for individual trees at each site). For example, at site O, strong negative correlations (0.80) were apparent on the northwest side of the tree patches in the southeast portion of the study area. 220 This is the area of site O where the north facing slope is likely the largest influence on snow depths. The high positive correlations between canopy edge and snow depth occur in the north where snow depths are low (less than 1 m). Site A also had negative correlations in the north/north-western sampled region, and we propose this is likely due to northeast winds and deeper snow depths in the northeast facing slopes in the southern portion of the site. We also found that single trees not belonging to a patch or trees in small patches (e.g. <10 trees surrounding), had negative correlations between canopy edge and 225 snow depth.

3.5 Influence of tree height and distance on snow depth

We found that the correlations of maximum tree height with snow depth are highest within 6 m, though several sites had the highest correlation at 3 to 4 m distance away from individual trees (Fig. B8). Site K had high correlation (0.56) at 1 m whereas site O had high correlation at 6 m (0.74). Overall sites M and N had relatively lower correlations (0.36 and 0.28, respectively) 230 with distance than the other sites. These sites both had the highest percent tree cover, though site M had tall trees (mean height of 21.6 m) and Site N had short trees (mean height of 10.5 m) (Table 1). Site A had a correlation of 0.6 at 4 m and site F had a correlation of 0.39 at 3 m.

3.6 Gap distribution

Our results show that site N has the largest median D/H ratio (0.74) compared to all other sites of <0.5 (Table 1). Site N is the 235 only site with a dispersed tree pattern (Fig. B9) and thus the most likely site to experience lower interception, possibly resulting in deeper snow.

3.7 Directional analysis

We found negative correlations between tree heights and snow depths based on direction at all sites (Table A3) and regardless of tree height for sites K, N, and O (Tables A4-5). We found positive correlations at site F in the south direction and site M in 240 the south and east directions for trees < 10m and in the west and south directions for site A for trees > 10 m (Tables A4-5). We found snow depths were different between the north and south sides of trees at sites A, K, and O but not for any other sites or directions (Table A6).

https://doi.org/10.5194/tc-2020-277
Preprint. Discussion started: 23 October 2020

4 Discussion

We observed several interesting relationships between vegetation canopies, topography, wind and snow depths across our sites. As expected, snow depths were deeper in the open compared to under canopy. However, describing the relationships between vegetation and snow is complicated by the structure, distribution (pattern), and type of vegetation. The relationship is further convoluted by local topography and wind speed/direction. For example, we found that slope, aspect, and wind (rather than vegetation) might control snow depths at local scales at two of the sites, A and O. This is not surprising, as site A was dominated by 0.4-0.6 m tall shrubs and wind exposed, and site O had a relatively low tree canopy cover. While site A had the lowest tree canopy cover in our dataset, we only sampled the edge of a much larger patch of trees (based on field observations). High snow depths were found in open northeast facing slopes at site A where wind deposits snow. Thus, local topographic interactions with wind have a major influence on snow accumulation, especially when we do not consider the much larger landscape controls. While sites A and O have slopes within the overall range of all of our sites, the combination of local slope and aspect for site O, appear to be driving factors in snow depths. In fact, site O has the highest mean snow depth (1.44 m), likely due to these local site conditions.

When our analyses were confined to under the canopy of individual trees, we generally found a significant relationship between the vertical spatial arrangement of the foliage (based on the FHD) and snow depth, but this relationship did not hold across all sites. For example, FHD explained less than 20 % of the variance of snow depth at site M. This site has the highest mean tree heights of the study. Taken together with a negative correlation between Zq90 and snow depth, the height of the tree likely had higher control on snow depths than on the particular foliar arrangement of the trees at this site. Overall, sites M and N had the lowest correlations between vegetation metrics and snow depth. This may be due to the vegetation patterns at these sites (under the canopy slope and aspect have no effect at both sites M and N (Table 3, Fig. 6a)). Site M is a relatively open area with mature Engelmann spruce and subalpine fir trees in the SW and NE areas of our site. Subalpine fir trees are generally more slender than Engelmann spruce, and thus their shape may not be as influential on accumulation of under canopy snow depths. Site N has the highest percent cover and the smallest trees (mean tree height 10.5 m, SD of 2.62 m, Table 1). This second growth canopy is the only site dominated by lodgepole pine, which are also slender. While the mean FHD is similar to the other sites, the spatial arrangement of the trees may have a larger control on snow depths. This is the only site with trees in a dispersed pattern in which the size of the gaps likely prevents snow interception, and thus provides an opportunity for snow accumulation. In fact, site N had the second highest mean snow depth under the canopy (1.38 m, compared with 1.44 m at site O, Table A2, Fig. 6a). Testing for a dispersed tree pattern could be beneficial to future studies, especially because previous research (e.g. Ning Sun et al., 2018) found gap size to be a control on snowmelt timing; however, our study was during the accumulation phase so we cannot draw similar conclusions for site N.

Similar to previous work (e.g. Moeser et al., 2015a; Mazzotti et al., 2019), we found that measures of distance from canopy are important correlates with snow depth. However, most of the previous work was performed with airborne lidar across larger spatial extents and lower vertical resolutions in the canopy. Our data are best suited to fine scale interactions between individual

https://doi.org/10.5194/tc-2020-277
Preprint. Discussion started: 23 October 2020

trees, or clusters of trees, and under the canopy or surrounding snow depths. Ultimately, understanding controls at the scale in which TLS provides is complementary to airborne lidar, which can help test larger scale features, such as gap area across space.

Our canopy edge analyses generally found that as the distance increases from the canopy edge, snow depths also increase. We also found that small patches or individual trees do not influence snow depths significantly with distance. In addition, on the north side of site A, wind and slope may influence the relationship between canopy edge and snow depths (where we found negative correlations, Fig. B2).

We did not find high snow depth accumulation or variability within a transition zone similar to the findings of Broxton et al. (2015). While their study included similar tree species, wind speeds and elevation, their spatial scale of analysis was larger with the use of airborne lidar. Interestingly, correlations between maximum tree height and snow depth in Grand Mesa occurs within 6 m of an individual tree at the sites, reinforcing local scale controls. Further, the negative correlations between snow depth and all cardinal directions from individual trees indicate that we should expect shallower snow within the 10 m transition zone from taller trees (Tables A3-5). In other words, two adjacent trees with different heights affect snow depth differently in any one direction and shorter trees keep deeper snow in all directions. We expected the opposite to occur i.e. taller trees should create larger shadows and provide more shading/sheltering. As our snow-on datasets are from the accumulation season, we may not see shading effects of taller trees in the transition zone; negligible melt had occurred at the time of these surveys. If our datasets extended throughout the season, we might expect these relationships to change. Note that due to sampling extent, our transition zone analysis was performed at 1 m increments instead of at multiples of mean tree height as in previous literature (e.g. Currier and Lundquist, 2018).

Following previous studies that showed a directional relationship with snow depths (e.g. Mazzotti et al., 2019; Currier and Lundquist, 2018), we found significantly different snow depths between the north and south sides of trees at site A, K, and O, but not other sites. This may be due to the local topography and wind at sites A and O. Site K had a maximum correlation between tree height and snow depth at 1m, and thus there may be local controls with distance and direction at site K. Additionally, previous lidar-based canopy snow interaction studies (Trujillo et al., 2007, 2009; Deems et al., 2006) relied on more simple canopy models using maximum height. Our results show that in nearly all situations, structural information contained in denser lidar point clouds have much more predictive capability.

5 Conclusions

Our study indicates that even with fine scale, individual tree observations from TLS, vegetation structural metrics are not enough to describe snow depth during the accumulation season. Local scale topography and wind should also be considered. While our sites were not designed solely for intercomparison, we found notable trends in our site comparisons. The vertical arrangement of foliage (e.g. FHD) of individual trees and tree height influences under canopy snow depths, and in some cases, quite strongly. Further studies should be designed to test this within and between species. For example, our sites were primarily

https://doi.org/10.5194/tc-2020-277
Preprint. Discussion started: 23 October 2020

Engleman spruce, subalpine fir, and lodgepole pine, all of which have different canopy structural shapes. Further studies targeting samples of each of these with different foliar arrangements and heights should be undertaken to fully understand the implications of FHD and tree heights on snow depths at local scales.

We also found that topography had greater control than vegetation at sites where slopes favored wind conditions for increasing snow depths, or where vegetation presence was minimal. While the latter may be obvious, increased observations with varying vegetation cover, wind, and topography should be considered with TLS.

This study highlights the complementary nature of TLS observations to airborne lidar, where TLS can provide fine scale observations within the canopy and relationships with under the canopy snow depth. Data from TLS can also be used to validate airborne lidar (e.g. Currier et al., 2019), and further studies should investigate how vegetation metrics such as FHD compare between TLS and airborne lidar in these snow-dominated forest ecosystems. Further, along with airborne lidar, TLS provides a complementary dataset for upscaling to similar types of vegetation structure and topography observed from satellites such as ICESat-2, or missions such as GEDI. Importantly, results from this study and others with TLS and airborne lidar for forest-snow observations can also be the foundation for the 2017 Decadal Survey designated observable, Surface Topography Vegetation study (National Academy of Sciences, Engineering, Medicine, 2018).

Data availability

The TLS data are from 2017 SnowEx campaign collected at Grand Mesa, Colorado and are accessible at https://nsidc.org/data/SNEX17_TLS_PC_BSU/versions/1 and https://nsidc.org/data/SNEX17_TLS_PC_CRREL/versions/1.

Author contribution

Zach Uhlmann, Lucas Spaete, Christopher A. Hiemstra, Christopher J. Tennant, Art Gelvin, and Nancy Glenn contributed field data collection. Lucas Spaete, Nancy Glenn, Christopher A. Hiemstra, Hans-Peter Marshall, and Art Gelvin designed the project. In addition, Zach Uhlmann, Nancy Glenn, Ahmad Hojatimalekshah, Christopher A. Hiemstra, Christopher J. Tennant, Jake Graham, Hans-Peter Marshall, Jim McNamara and Josh Enterkine contributed in writing and interpretations. Ahmad Hojatimalekshah did the analysis.

The authors declare that they have no conflict of interest.

Acknowledgements

Funding and support for the project was provided by NASA Awards 80NSSC18K0955 and NNX17AL61G, NASA SnowEx 2017 campaign, and the Department of Geosciences, Boise State University. We would like to thank all those who participated and supported the NASA 2017 SnowEx campaign.

https://doi.org/10.5194/tc-2020-277
Preprint. Discussion started: 23 October 2020

References

Bewley, D., Alila, Y. and Varhola, A.: Variability of snow water equivalent and snow energetics across a large catchment subject to Mountain Pine Beetle infestation and rapid salvage logging, Journal of Hydrology, 388(3–4), 464–479, doi:10.1016/j.jhydrol.2010.05.031, 2010.

Blöschl, G.: Scaling in hydrology, Hydrol. Process., 15(4), 709–711, doi:10.1002/hyp.432, 2001.

Broxton, P. D., Harpold, A. A., Biederman, J. A., Troch, P. A., Molotch, N. P. and Brooks, P. D.: Quantifying the effects of vegetation structure on snow accumulation and ablation in mixed-conifer forests, Ecohydrol., 8(6), 1073–1094, doi:10.1002/eco.1565, 2015.

Currier, W. R. and Lundquist, J. D.: Snow Depth Variability at the Forest Edge in Multiple Climates in the Western United States, Water Resour. Res., 54(11), 8756–8773, doi:10.1029/2018WR022553, 2018.

Currier, W. R., Pflug, J., Mazzotti, G., Jonas, T., Deems, J. S., Bormann, K. J., Painter, T. H., Hiemstra, C. A., Gelvin, A., Uhlmann, Z., Spaete, L., Glenn, N. F. and Lundquist, J. D.: Comparing Aerial Lidar Observations With Terrestrial Lidar and Snow-Probe Transects From NASA's 2017 SnowEx Campaign, Water Resour. Res., 55(7), 6285–6294, doi:10.1029/2018WR024533, 2019.

Deems, J. S., Fassnacht, S. R. and Elder, K. J.: Fractal Distribution of Snow Depth from Lidar Data, Journal of Hydrometeorology, 7(2), 285–297, doi:10.1175/JHM487.1, 2006.

Deems, J. S., Painter, T. H. and Finnegan, D. C.: Lidar measurement of snow depth: a review, J. Glaciol., 59(215), 467–479, doi:10.3189/2013JoG12J154, 2013.

Dickerson-Lange, S. E., Lutz, J. A., Gersonde, R., Martin, K. A., Forsyth, J. E. and Lundquist, J. D.: Observations of distributed snow depth and snow duration within diverse forest structures in a maritime mountain watershed, Water Resour. Res., 51(11), 9353–9366, doi:10.1002/2015WR017873, 2015.

Gauthier, S., Bernier, P., Kuuluvainen, T., Shvidenko, A. Z. and Schepaschenko, D. G.: Boreal forest health and global change, Science, 349(6250), 819–822, doi:10.1126/science.aaa9092, 2015.

Gleason, K. E., Nolin, A. W. and Roth, T. R.: Charred forests increase snowmelt: Effects of burned woody debris and incoming solar radiation on snow ablation, Geophys. Res. Lett., 40(17), 4654–4661, doi:10.1002/grl.50896, 2013.

Glenn, N., Spaete, L., Uhlmann, Z., Merriman, C., Raymondi, A., and Tennant, C.: SnowEx17 Boise State University Terrestrial Laser Scanner (TLS) Point Cloud, Version 1, doi:10.5067/IWGD4WFMCQNW, 2019.

Grünewald, T., Schirmer, M., Mott, R. and Lehning, M.: Spatial and temporal variability of snow depth and ablation rates in a small mountain catchment, The Cryosphere, 4(2), 215–225, doi:10.5194/tc-4-215-2010, 2010.

Güntner, A., Stuck, J., Werth, S., Döll, P., Verzano, K. and Merz, B.: A global analysis of temporal and spatial variations in continental water storage, Water Resour. Res., 43(5), doi:10.1029/2006WR005247, 2007.

Hall, D. K., Riggs, G. A. and Salomonson, V. V.: Development of methods for mapping global snow cover using moderate resolution imaging spectroradiometer data, Remote Sensing of Environment, 54(2), 127–140, doi:10.1016/0034-4257(95)00137-P, 1995.

Hartzell, P. J., Gadomski, P. J., Glennie, C. L., Finnegan, D. C. and Deems, J. S.: Rigorous error propagation for terrestrial laser scanning with application to snow volume uncertainty, J. Glaciol., 61(230), 1147–1158, doi:10.3189/2015JoG15J031, 2015.

Hedrick, A. R., Marks, D., Havens, S., Robertson, M., Johnson, M., Sandusky, M., Marshall, H., Kormos, P. R., Bormann, K. J. and Painter, T. H.: Direct Insertion of NASA Airborne Snow Observatory-Derived Snow Depth Time Series Into the iSnobal Energy Balance Snow Model, Water Resour. Res., 54(10), 8045–8063, doi:10.1029/2018WR023190, 2018.

Hedstrom, N. R. and Pomeroy, J. W.: Measurements and modelling of snow interception in the boreal forest, Hydrological Processes, 12(10–11), 1611–1625, doi:10.1002/(SICI)1099-1085(199808/09)12:10/11<1611::AID-HYP684>3.0.CO;2-4, 1998.

Hiemstra, C.: SnowEx17 CRREL Terrestrial Laser Scanner (TLS) Point Cloud, Version 1, doi:10.5067/YOIPYEWCZOD5, 2017.

Homan, J. W., Luce, C. H., McNamara, J. P. and Glenn, N. F.: Improvement of distributed snowmelt energy balance modeling with MODIS-based NDSI-derived fractional snow-covered area data, Hydrol. Process., 25(4), 650–660, doi:10.1002/hyp.7857, 2011.

Hopkinson, C., Sitar, M., Chasmer, L. and Treitz, P.: Mapping Snowpack Depth beneath Forest Canopies Using Airborne Lidar, photogramm eng remote sensing, 70(3), 323–330, doi:10.14358/PERS.70.3.323, 2004.

Kim, E., Gatebe, C., Hall, D., Newlin, J., Misakonis, A., Elder, K., Marshall, H. P., Hiemstra, C., Brucker, L., De Marco, E., Crawford, C., Kang, D. H. and Entin, J.: NASA's snowex campaign: Observing seasonal snow in a forested environment, in 2017 IEEE International Geoscience and Remote Sensing Symposium (IGARSS), pp. 1388–1390, IEEE, Fort Worth, TX., 2017.

Lague, D., Brodu, N. and Leroux, J.: Accurate 3D comparison of complex topography with terrestrial laser scanner: Application to the Rangitikei canyon (N-Z), ISPRS Journal of Photogrammetry and Remote Sensing, 82, 10–26, doi:10.1016/j.isprsjprs.2013.04.009, 2013.

Luce, C. H., Tarboton, D. G. and Cooley, K. R.: Sub-grid parameterization of snow distribution for an energy and mass balance snow cover model, Hydrological Processes, 13(12–13), 1921–1933, doi:10.1002/(SICI)1099-1085(199909)13:12/13<1921::AID-HYP867>3.0.CO;2-S, 1999.

Mazzotti, G., Currier, W. R., Deems, J. S., Pflug, J. M., Lundquist, J. D. and Jonas, T.: Revisiting Snow Cover Variability and Canopy Structure Within Forest Stands: Insights From Airborne Lidar Data, Water Resour. Res., 55(7), 6198–6216, doi:10.1029/2019WR024898, 2019.

Moeser, D., Stähli, M. and Jonas, T.: Improved snow interception modeling using canopy parameters derived from airborne LiDAR data, Water Resour. Res., 51(7), 5041–5059, doi:10.1002/2014WR016724, 2015a.

https://doi.org/10.5194/tc-2020-277
Preprint. Discussion started: 23 October 2020

Moeser, D., Morsdorf, F. and Jonas, T.: Novel forest structure metrics from airborne LiDAR data for improved snow interception estimation, Agricultural and Forest Meteorology, 208, 40–49, doi:10.1016/j.agrformet.2015.04.013, 2015b.

National Academies of Sciences, E.: Thriving on Our Changing Planet: A Decadal Strategy for Earth Observation from Space., 2018.

Nolin, A. W. and Daly, C.: Mapping "At Risk" Snow in the Pacific Northwest, Journal of Hydrometeorology, 7(5), 1164–1171, doi:10.1175/JHM543.1, 2006.

Painter, T. H., Berisford, D. F., Boardman, J. W., Bormann, K. J., Deems, J. S., Gehrke, F., Hedrick, A., Joyce, M., Laidlaw, R., Marks, D., Mattmann, C., McGurk, B., Ramirez, P., Richardson, M., Skiles, S. M., Seidel, F. C. and Winstral, A.: The Airborne Snow Observatory: Fusion of scanning lidar, imaging spectrometer, and physically-based modeling for mapping snow water equivalent and snow albedo, Remote Sensing of Environment, 184, 139–152, doi:10.1016/j.rse.2016.06.018, 2016.

Pomeroy, J. W., Marks, D., Link, T., Ellis, C., Hardy, J., Rowlands, A. and Granger, R.: The impact of coniferous forest temperature on incoming longwave radiation to melting snow, Hydrol. Process., 23(17), 2513–2525, doi:10.1002/hyp.7325, 2009.

R: The R Project for Statistical Computing, [online] Available from: https://www.r-project.org/ (Accessed 16 September 2020).

Raleigh, M. S., Rittger, K., Moore, C. E., Henn, B., Lutz, J. A. and Lundquist, J. D.: Ground-based testing of MODIS fractional snow cover in subalpine meadows and forests of the Sierra Nevada, Remote Sensing of Environment, 128, 44–57, doi:10.1016/j.rse.2012.09.016, 2013.

Revuelto, J., López-Moreno, J. I., Azorin-Molina, C. and Vicente-Serrano, S. M.: Canopy influence on snow depth distribution in a pine stand determined from terrestrial laser data: Canopy influence on snow depth distribution, Water Resour. Res., 51(5), 3476–3489, doi:10.1002/2014WR016496, 2015.

Revuelto, J., Vionnet, V., López-Moreno, J.-I., Lafaysse, M. and Morin, S.: Combining snowpack modeling and terrestrial laser scanner observations improves the simulation of small scale snow dynamics, Journal of Hydrology, 533, 291–307, doi:10.1016/j.jhydrol.2015.12.015, 2016a.

Revuelto, J., López-Moreno, J.-I., Azorin-Molina, C., Alonso-González, E. and Sanmiguel-Vallelado, A.: Small-Scale Effect of Pine Stand Pruning on Snowpack Distribution in the Pyrenees Observed with a Terrestrial Laser Scanner, Forests, 7(12), 166, doi:10.3390/f7080166, 2016b.

Roussel, J.-R., documentation), D. A. (Reviews the, features), F. D. B. (Fixed bugs and improved catalog, segment_snags()), A. S. M. (Implemented wing2015() for, track_sensor()), B. J.-F. (Contributed to R. for and track_sensor()), G. D. (Implemented G. for: lidR: Airborne LiDAR Data Manipulation and Visualization for Forestry Applications. [online] Available from: https://CRAN.R-project.org/package=lidR (Accessed 16 September 2020), 2020.

Rutter, N., Essery, R., Pomeroy, J., Altimir, N., Andreadis, K., Baker, I., Barr, A., Bartlett, P., Boone, A., Deng, H., Douville, H., Dutra, E., Elder, K., Ellis, C., Feng, X., Gelfan, A., Goodbody, A., Gusev, Y., Gustafsson, D., Hellström, R., Hirabayashi, Y., Hirota, T., Jonas, T., Koren, V., Kuragina, A., Lettenmaier, D., Li, W.-P., Luce, C., Martin, E., Nasonova, O., Pumpanen,

J., Pyles, R. D., Samuelsson, P., Sandells, M., Schädler, G., Shmakin, A., Smirnova, T. G., Stähli, M., Stöckli, R., Strasser, U., Su, H., Suzuki, K., Takata, K., Tanaka, K., Thompson, E., Vesala, T., Viterbo, P., Wiltshire, A., Xia, K., Xue, Y. and Yamazaki, T.: Evaluation of forest snow processes models (SnowMIP2), J. Geophys. Res., 114(D6), D06111, doi:10.1029/2008JD011063, 2009.

Schirmer, M., Wirz, V., Clifton, A. and Lehning, M.: Persistence in intra-annual snow depth distribution: 1. Measurements and topographic control, 1, Water Resour. Res., 47(9), doi:10.1029/2010WR009426, 2011.

Seyednasrollah, B. and Kumar, M.: Net radiation in a snow-covered discontinuous forest gap for a range of gap sizes and topographic configurations, J. Geophys. Res. Atmos., 119(17), 10,323-10,342, doi:10.1002/2014JD021809, 2014.

Seyednasrollah, B., Kumar, M. and Link, T. E.: On the role of vegetation density on net snow cover radiation at the forest floor, J. Geophys. Res. Atmos., 118(15), 8359–8374, doi:10.1002/jgrd.50575, 2013.

Sicart, J. E., Essery, R. L. H., Pomeroy, J. W., Hardy, J., Link, T. and Marks, D.: A Sensitivity Study of Daytime Net Radiation during Snowmelt to Forest Canopy and Atmospheric Conditions, J. Hydrometeor., 5(5), 774–784, doi:10.1175/1525-7541(2004)005<0774:ASSODN>2.0.CO;2, 2004.

Sun, N., Wigmosta, M., Zhou, T., Lundquist, J., Dickerson-Lange, S. and Cristea, N.: Evaluating the functionality and streamflow impacts of explicitly modelling forest-snow interactions and canopy gaps in a distributed hydrologic model, Hydrological Processes, 32(13), 2128–2140, doi:10.1002/hyp.13150, 2018.

Tennant, C. J., Harpold, A. A., Lohse, K. A., Godsey, S. E., Crosby, B. T., Larsen, L. G., Brooks, P. D., Van Kirk, R. W. and Glenn, N. F.: Regional sensitivities of seasonal snowpack to elevation, aspect, and vegetation cover in western North America, Water Resour. Res., 53(8), 6908–6926, doi:10.1002/2016WR019374, 2017.

Troendle, C. A. and King, R. M.: The Effect of Timber Harvest on the Fool Creek Watershed, 30 Years Later, Water Resour. Res., 21(12), 1915–1922, doi:10.1029/WR021i012p01915, 1985.

Trujillo, E., Ramírez, J. A. and Elder, K. J.: Topographic, meteorologic, and canopy controls on the scaling characteristics of the spatial distribution of snow depth fields, Water Resour. Res., 43(7), doi:10.1029/2006WR005317, 2007.

Trujillo, E., Ramírez, J. A. and Elder, K. J.: Scaling properties and spatial organization of snow depth fields in sub-alpine forest and alpine tundra, Hydrol. Process., 23(11), 1575–1590, doi:10.1002/hyp.7270, 2009.

Winstral, A., Marks, D. and Gurney, R.: Simulating wind-affected snow accumulations at catchment to basin scales, Advances in Water Resources, 55, 64–79, doi:10.1016/j.advwatres.2012.08.011, 2013.

Zheng, Z., Kirchner, P. B. and Bales, R. C.: Topographic and vegetation effects on snow accumulation in the southern Sierra Nevada: a statistical summary from lidar data, The Cryosphere, 10(1), 257–269, doi:10.5194/tc-10-257-2016, 2016.

https://doi.org/10.5194/tc-2020-277
Preprint. Discussion started: 23 October 2020

The Cryosphere
Discussions
Open Access
EGU

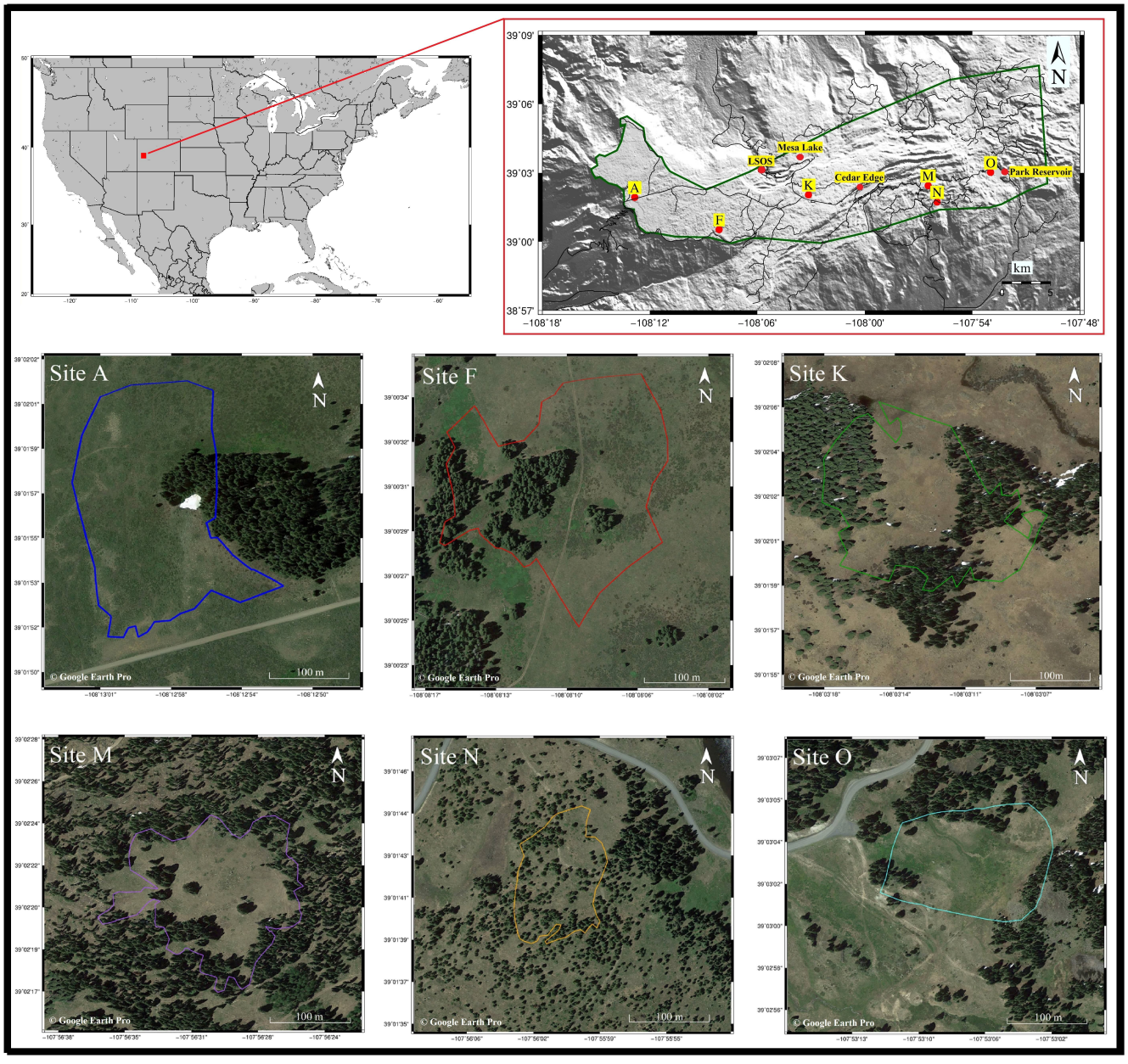

Figure 1: Study area and location of TLS sites and meteorological stations.

https://doi.org/10.5194/tc-2020-277
Preprint. Discussion started: 23 October 2020

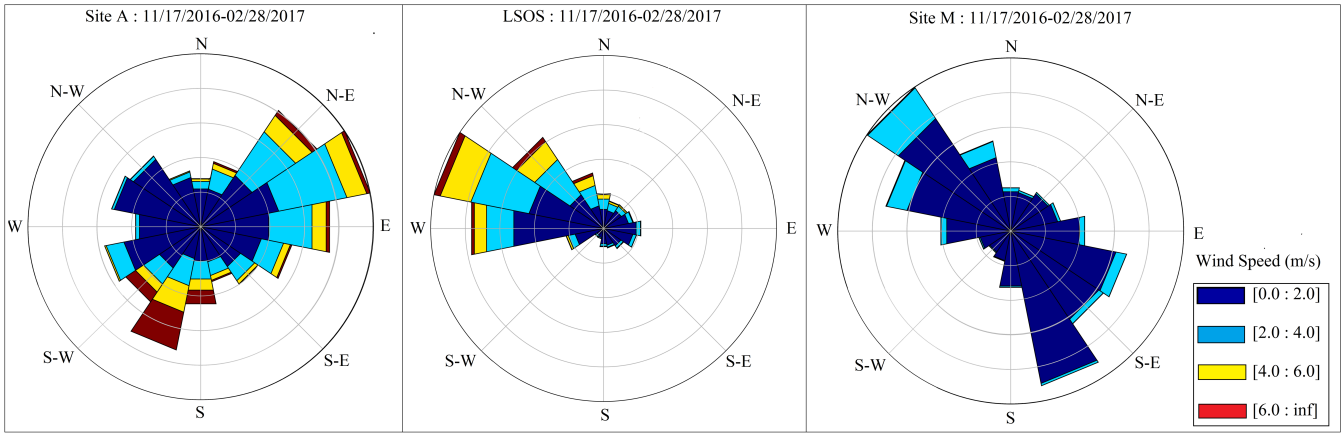

Figure 2: Rose diagrams of meteorological stations A, LSOS, and M.

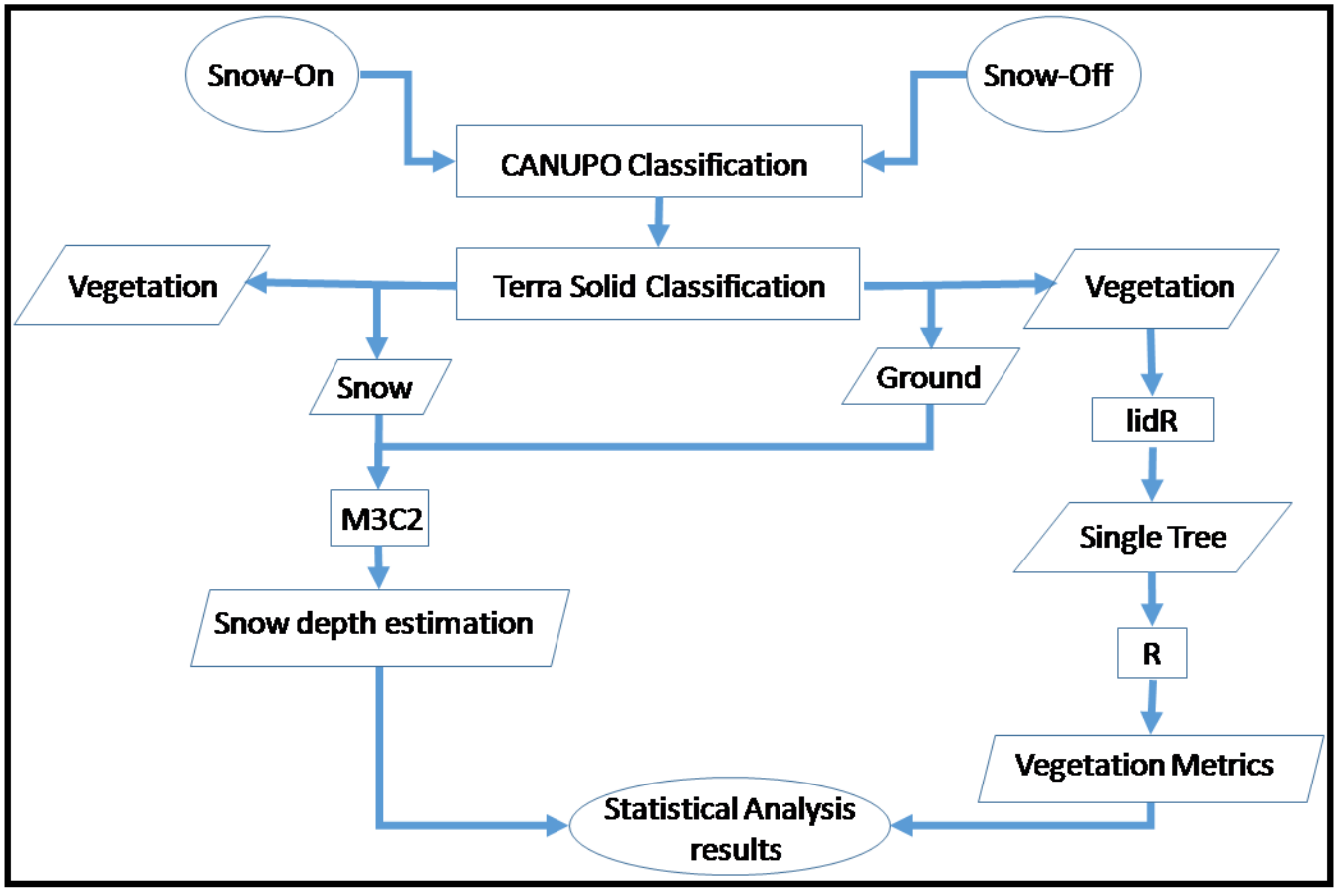

Figure 3: TLS data processing workflow.

https://doi.org/10.5194/tc-2020-277
Preprint. Discussion started: 23 October 2020

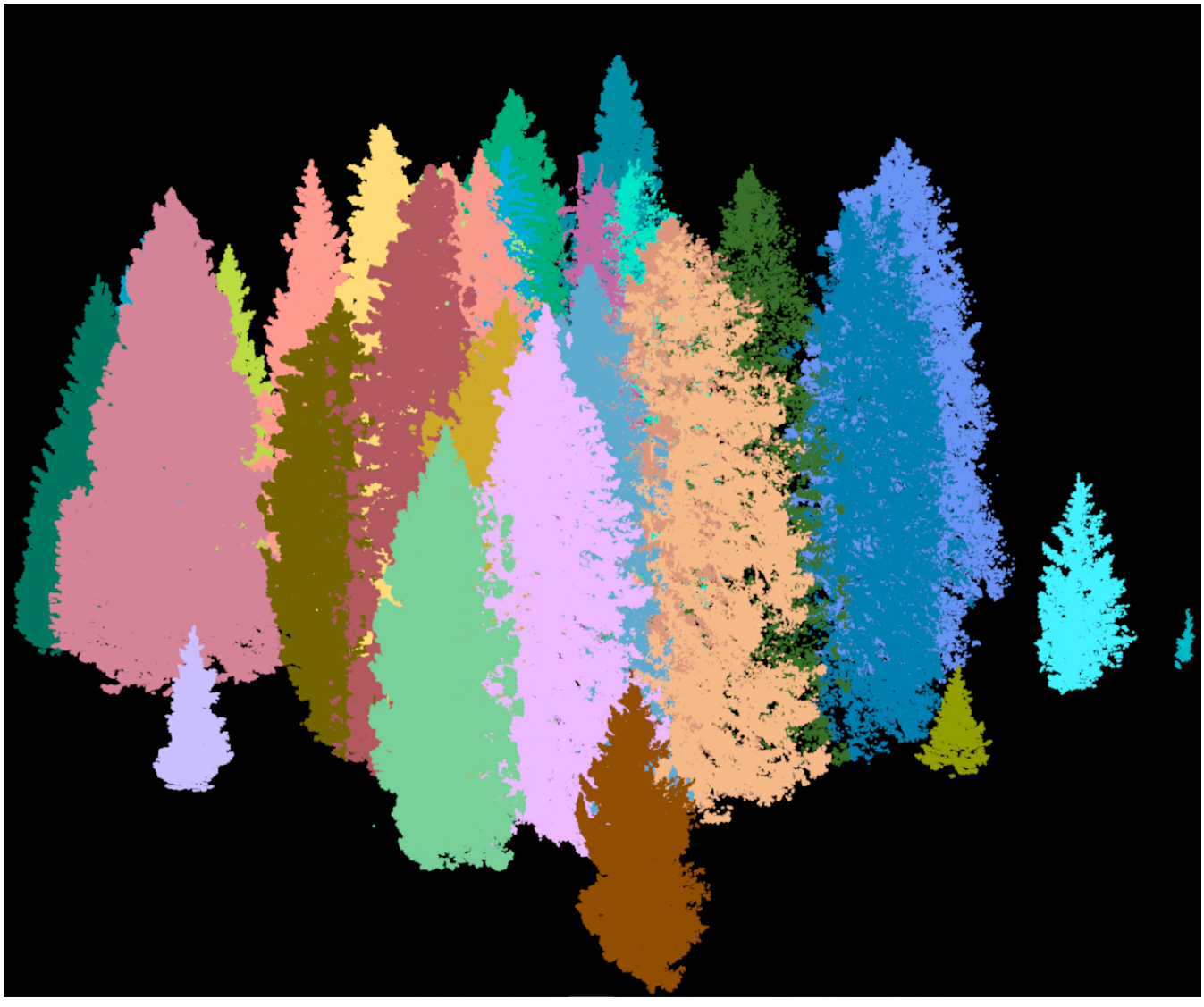

Figure 4: As an example, segmentation results for one las tile at site F.

https://doi.org/10.5194/tc-2020-277
Preprint. Discussion started: 23 October 2020

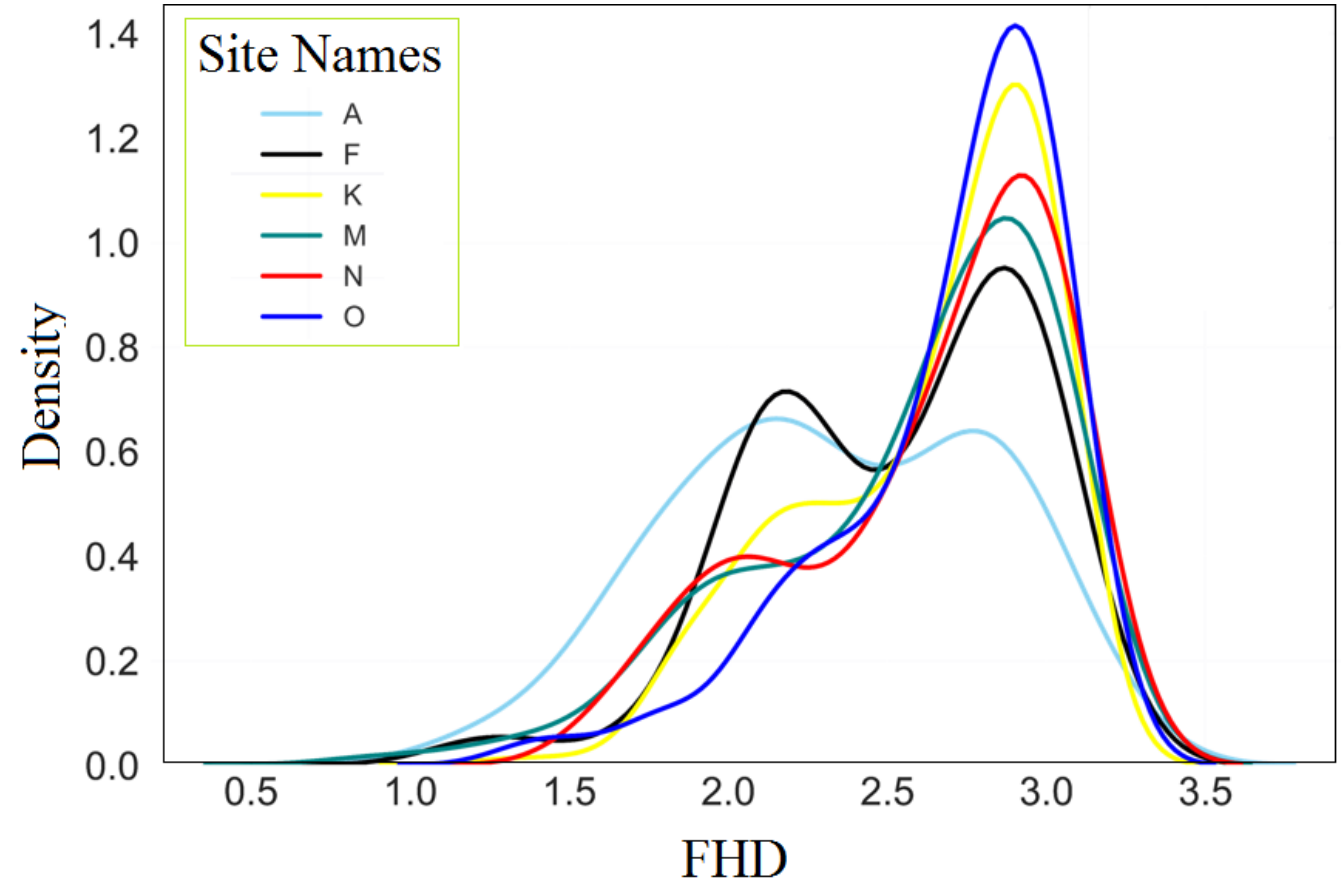

Figure 5: Foliage Height Diversity (FHD) distribution for each site.

https://doi.org/10.5194/tc-2020-277
Preprint. Discussion started: 23 October 2020

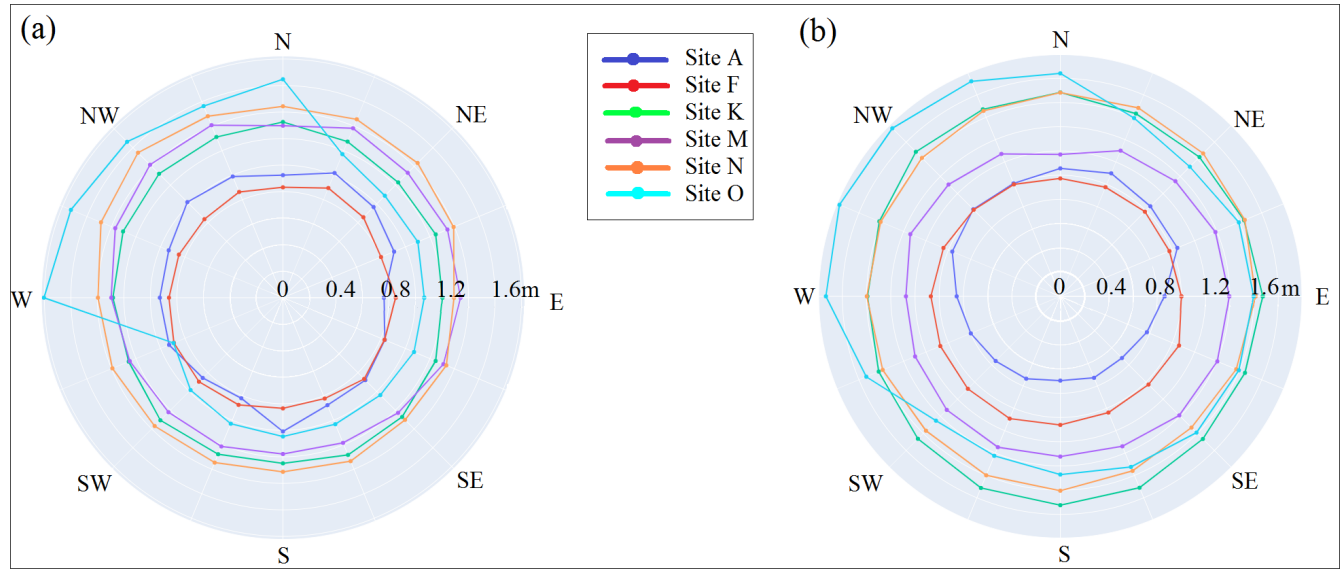

475 **Figure 6: Under the canopy (a) and open area (b) snow depth at different aspects.**

https://doi.org/10.5194/tc-2020-277
Preprint. Discussion started: 23 October 2020

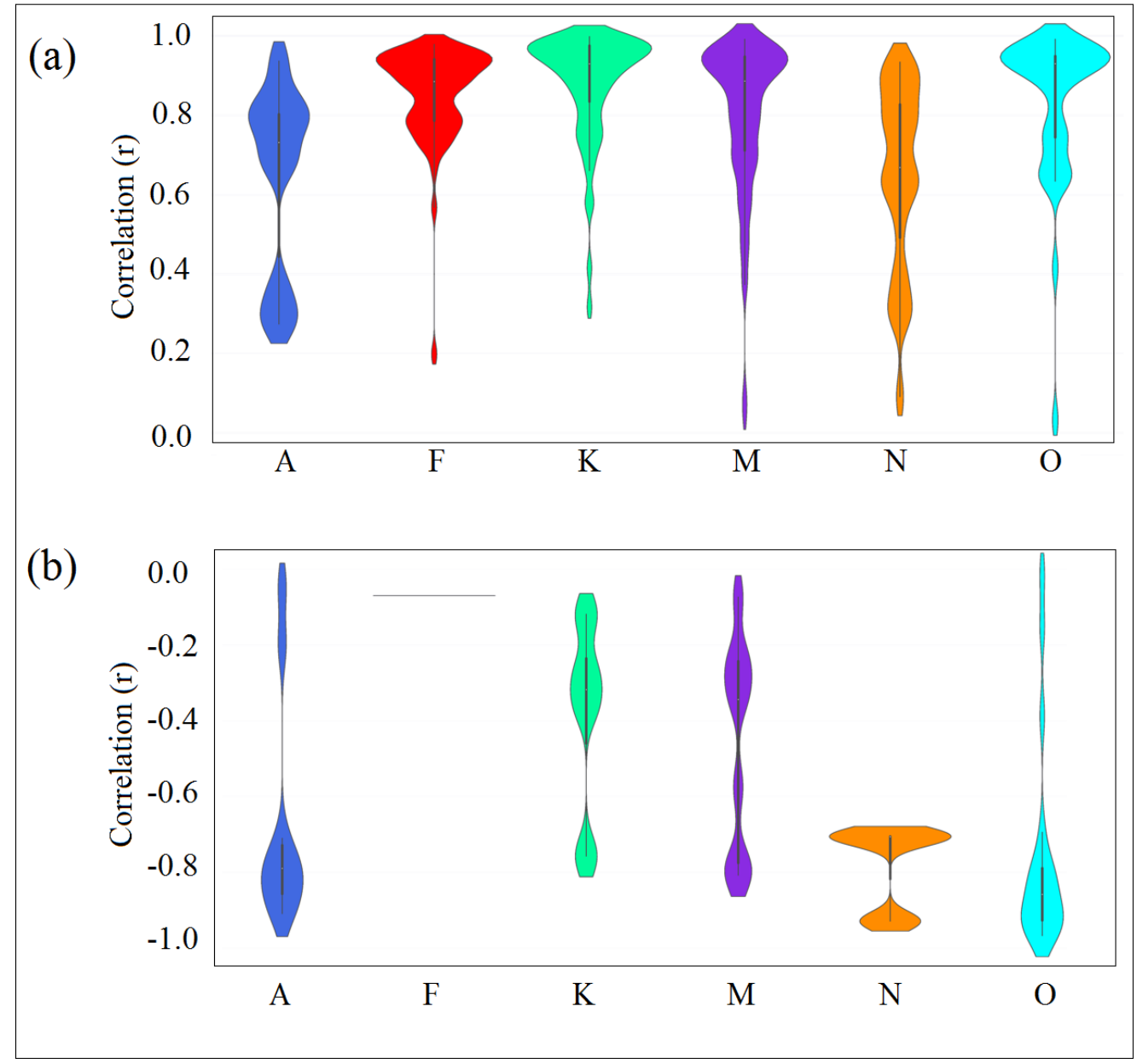

Figure 7: Snow depth correlation for each site with the distance from the edge. Positive correlations are shown in (a) and negative correlations in (b).

https://doi.org/10.5194/tc-2020-277
Preprint. Discussion started: 23 October 2020


The Cryosphere Discussions

480 **Table 1. Terrestrial laser scanning site descriptions. Sd = standard deviation. D/H = Distance/Height. FHD = foliar height diversity (described below).**

Site	Area of Analysis (m^2)	Mean Elevation (m) (sd)	Elevation Range (m)	Wind Direction	Vegetation Type	Tree % Cover	D/H	Range of Tree Height (m)	Mean Tree Height (m) (sd)	Median FHD (m) (sd)	Comments
A	29128	3037 (3.6)	3027-3045	Westerly	Mostly Shrubs with Engelmann Spruce	9 %	0.36	2-27	16.6(5.77)	2.27(0.48)	Sampled edge of larger tree cover extent.
F	37838	3105 (6.6)	3090-3118	…	Engelmann Spruce	24 %	0.32	2-29.2	21.4(6.38)	2.64(0.42)	Patchy Dense Trees.
K	31497	3253 (1.4)	3249-3257	…	Engelmann Spruce	38 %	0.41	1.7-30	18.7(6.45)	2.75(0.38)	Patchy Trees.
M	21994	3122 (4.7)	3114-3142	NW to SE	Engelmann Spruce	45 %	0.39	5.7-33.7	21.6(7.45)	2.7(0.46)	Patchy Trees.
N	10187	3054 (2.4)	3047-3061	…	Lodge Pole Pine	52 %	0.74	1.7-28.3	10.5(2.62)	2.77(0.42)	Second-growth, dispersed Lodge Pole Pine.
O	24302	3067 (4.0)	3055-3078	…	Subalpine Meadow with Engelmann Spruce	14 %	0.39	5-33.4	16.4(7.65)	2.82(0.37)	Two main slopes, one towards the south and other towards the NW. The later has the deepest snow.

Table 2. Vegetation metrics derived for individual trees at each of the sites. Where appropriate, equations are presented in Table A1.

Vegetation metrics			
Maximum height **(Zmax)**	Mean height **(Zmean)**	Minimum height **(Zmin)**	Height std **(Zstd)**
Height variance **(Zvar)**	Height range **(Zhgt_rng)**	Skewness **(Zskew)**	Kurtosis **(Zkurt)**
Crown volume **(crwnvlm)**	Crown surface **(crwnsrf)**	Median Absolute Deviation **(MAD)** from Median Height	Mean Absolute Deviation **(AAD)** from Mean Height

https://doi.org/10.5194/tc-2020-277
Preprint. Discussion started: 23 October 2020

Canopy relief ratio **(CRR)**	Hull surface area **(cnvhll_area)**	Percentage of returns above mean height **(pzbvzmn)**	Percentage of returns above 1m **(pzabov1)**
Percentile (quantile) of height distribution **(zq*)**	Cumulative percentage of return in the xth layer **(zpcum*)**	Number of LiDAR Vegetation Returns **(nV)**	Number of Lidar Ground Returns **(nG)**
Height Coefficient of Variation **(Zcv)**	Foliage Height Diversity **(FHD)**		

485

Table 3. Correlations between snow depth and slope and aspect in the open areas and within the canopy; and between snow depth and vegetation metrics (highest and 2nd highest correlations are shown). It worth mentioning that slope angles at Grand Mesa are small compared to many mountain environments.

Site	Correlation with slope (open area)	Correlation with slope (sub-canopy)	Correlation with aspect (open area)	Correlation with aspect (sub-canopy)	Highest correlation with veg metric	2nd highest correlation with veg metric
A	0.44	0.0	-0.02	0.0	Pzabove1(-0.68)	FHD(-0.47)
F	0.11	0.0	0.02	0.0	FHD(-0.5)	Pzabove3(-0.48)
K	-0.22	-0.13	0.0	0.09	FHD(-0.46)	Zmax(-0.43)
M	-0.026	-0.046	-0.03	0.0	Zq90(-0.16)	Pzabove4(-0.13)
N	0.13	0.07	-0.07	0.09	FHD(-0.35)	Pzabove3(-0.35)
O	0.17	0.66	0.29	0.59	FHD(-0.75)	Zq95(-0.75)

Pzabove(x) = Percentage of returns above "x" meters; FHD = Foliage Height Diversity, all points; Zq(x) = Percentage (quantile) of height distribution; Zmax = Maximum Tree Height

https://doi.org/10.5194/tc-2020-277
Preprint. Discussion started: 23 October 2020

The Cryosphere Discussions
Open Access
EGU

Appendix A

Table A1. Vegetation metrics with equations and references

Vegetation Metric	Equation (Reference: BCAL Lidar Tools, Boise State University, Department of Geosciences, URL: https://github.com/bcal-lidar/tools)
Median Absolute Deviation (MAD) from Median Height	1.4826 x median(|height - median height|)
Mean Absolute Deviation (AAD) from Mean Height	mean(|height - mean height|)
Number of LiDAR Vegetation Returns (nV)	The total number of all the points within each pixel that are above the specified crown threshold value (CT=2m).
Number of LiDAR Ground Returns (nG)	The total number of all the points within each pixel that are below the specified ground threshold value (GT=0.5m)
Canopy Relief Ratio(CRR)	Canopy relief ratio = $((H_{MEAN} - H_{MIN}))/((H_{MAX} - H_{MIN}))$
Foliage Height Diversity (FHD)-All points	$FHD = -\sum P_i \ln(P_i)$ Where P_i is the proportion of the number of lidar returns in the ith layer to the sum of lidar points of all the layers (using all points) (bcal lidar tools documentation)
	Code and References
Hull surface area (cnvhll_area)	R 3.5.3 (R Core Team, 2019), lidR (*v3.1.1*; Roussel) package
Crown volume (crwnvlm)	R 3.5.3 (R Core Team, 2019), rLiDAR (*v0.1.1*; Silva) package
Crown surface (crwnsrf)	R 3.5.3 (R Core Team, 2019), rLiDAR (*v0.1.1*; Silva) package

Table A2. Snow depth under the canopy, within the 10 m transition zone, and in the open. The mean, standard deviation, minimum, 25-75 % percentiles, and maximum snow depths are shown for each site. Count is number of 0.5 m pixels.

	Canopy A	Transition A	Open A	Canopy F	Transition F	Open F
count	5462	43873	3311	1089	9341	674
mean	0.81	0.82	1.01	0.93	0.96	1.17
std	0.21	0.21	0.53	0.13	0.12	0.17
min	0.41	0.34	0.07	0.58	0.58	0.60
25 %	0.68	0.69	0.65	0.85	0.87	1.05
50 %	0.78	0.78	0.90	0.93	0.95	1.20
75 %	0.92	0.91	1.23	1.02	1.05	1.30
max	4.42	4.94	4.94	1.54	1.60	1.53

https://doi.org/10.5194/tc-2020-277
Preprint. Discussion started: 23 October 2020

	Canopy K	Transition K	Open K	Canopy M	Transition M	Open M
count	1493	11346	1206	5215	32252	12817
mean	1.31	1.32	1.59	1.19	1.28	1.53
std	0.17	0.17	0.24	0.18	0.21	0.16
min	0.78	0.78	0.72	0.16	0.09	0.04
25 %	1.22	1.23	1.42	1.10	1.15	1.46
50 %	1.30	1.30	1.64	1.19	1.25	1.53
75 %	1.41	1.42	1.75	1.27	1.41	1.61
max	2.53	2.53	3.10	4.12	3.71	1.91

	Canopy N	Transition N	Open N	Canopy O	Transition O	Open O
count	777	6064	491	75	107	1001
mean	1.38	1.40	1.61	1.44	1.50	1.62
std	0.21	0.18	0.17	0.38	0.36	0.15
min	0.81	0.81	0.81	0.89	0.89	0.89
25 %	1.25	1.28	1.50	1.13	1.18	1.56
50 %	1.37	1.38	1.64	1.36	1.44	1.63
75 %	1.47	1.49	1.72	1.70	1.76	1.69
max	2.57	2.57	2.30	2.23	2.28	2.45

495 **Table A3. Correlations between trees and snow depth (within a 10 m transition zone) based on cardinal direction. The columns are site, correlation, tree height range, and number of trees. Ranges of tree heights vary within sites because not all trees had adequate snow samples to test in all cardinal directions.**

Site	North	Tree height range (m)	# of trees	West	Tree height range (m)	# of trees	South	Tree height range (m)	# of trees	East	Tree height range (m)	# of trees
A	-0.53	2.05– 25.52	95	-0.46	2.05– 28.05	91	-0.40	2.05– 28.05	94	-0.34	2.05–28.05	101
F	-0.31	1.80– 29.31	212	-0.48	1.80– 28.59	213	-0.34	1.80–28.76	222	-0.29	1.80–29.31	214
K	-0.41	1.51 – 29.34	486	-0.34	1.51 – 29.34	485	-0.39	1.51– 29.97	474	-0.42	1.51–29.97	483
M	-0.12	5.23– 33.69	254	-0.14	5.72– 33.69	248	-0.25	5.23– 33.69	230	-0.09	5.23–33.69	241
N	-0.32	1.74– 19.83	237	-0.26	1.74 – 19.83	242	-0.30	1.77– 19.83	243	-0.22	1.74–28.34	232
O	-0.54	5.46– 33.42	122	-0.69	5.09– 33.42	127	-0.67	5.09– 33.42	133	-0.64	5.46– 32.46	131

Table A4. Same as Table A3 but for trees shorter than 10 m.

Site	North	# of trees	West	# of trees	South	# of trees	East	# of trees

https://doi.org/10.5194/tc-2020-277
Preprint. Discussion started: 23 October 2020


The Cryosphere Discussions

A	-0.7	21	-0.66	18	-0.88	16	-0.59	20
F	-0.41	34	-0.20	35	0.12	34	-0.23	32
K	-0.17	103	-0.18	101	-0.13	103	-0.24	106
M	-0.00	26	0.16	25	0.25	25	0.16	28
N	-0.37	89	-0.19	93	-0.22	91	-0.18	90
O	-0.25	33	-0.29	33	-0.15	41	-0.39	41

Table A5. Same as Table A3 but for trees taller than 10 m.

Site	North	# of trees	West	# of trees	South	# of trees	East	# of trees
A	-0.06	74	0.2	73	0.15	78	-0.1	71
F	-0.2	178	-0.46	178	-0.27	188	-0.17	182
K	-0.24	383	-0.18	384	-0.22	371	-0.18	377
M	-0.13	228	-0.18	223	-0.21	205	-0.02	213
N	-0.15	148	-0.12	149	-0.15	152	-0.05	142
O	-0.44	89	-0.52	94	-0.53	92	-0.51	90

Table A6: Wilcoxon signed-rank test results for comparing snow depth on the north and south sides (and east and west) for individual trees at each site. Note only trees that have snow depth data on both north and south or east and west are considered. Statistically significant are bolded.

Site	P-value (North-South)	Number of Samples	P-value (East-West)	Number of Samples
A	0.0004484	59	0.3498	60
F	0.807	138	0.704	130
K	0.0348	390	0.78	397
M	0.65	170	0.78	163
N	0.72	202	0.495	195
O	0.024	90	0.43	94

https://doi.org/10.5194/tc-2020-277
Preprint. Discussion started: 23 October 2020

The Cryosphere Discussions
Open Access
EGU

Appendix B

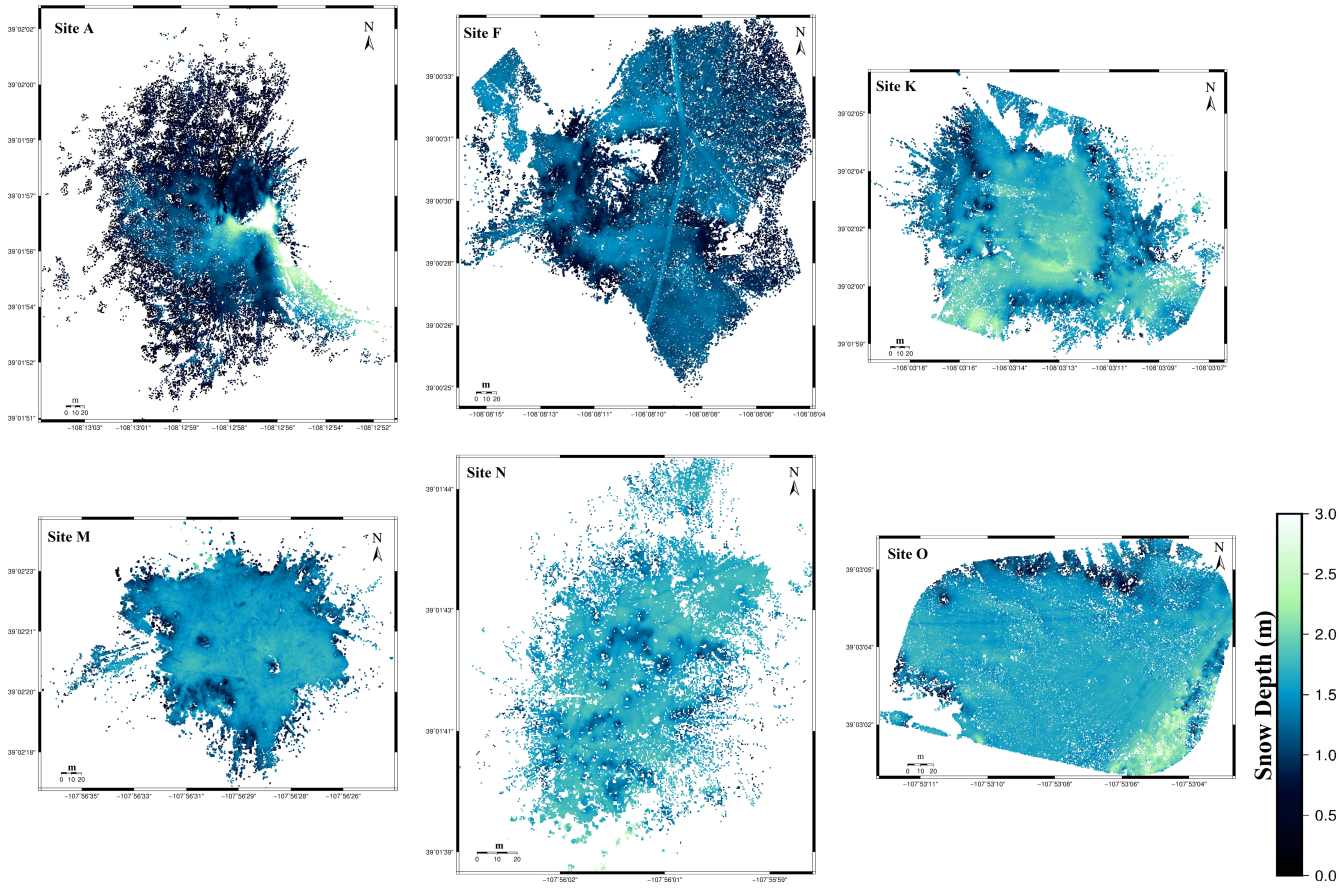

Figure B1: Snow depths at each site from TLS data.

https://doi.org/10.5194/tc-2020-277
Preprint. Discussion started: 23 October 2020

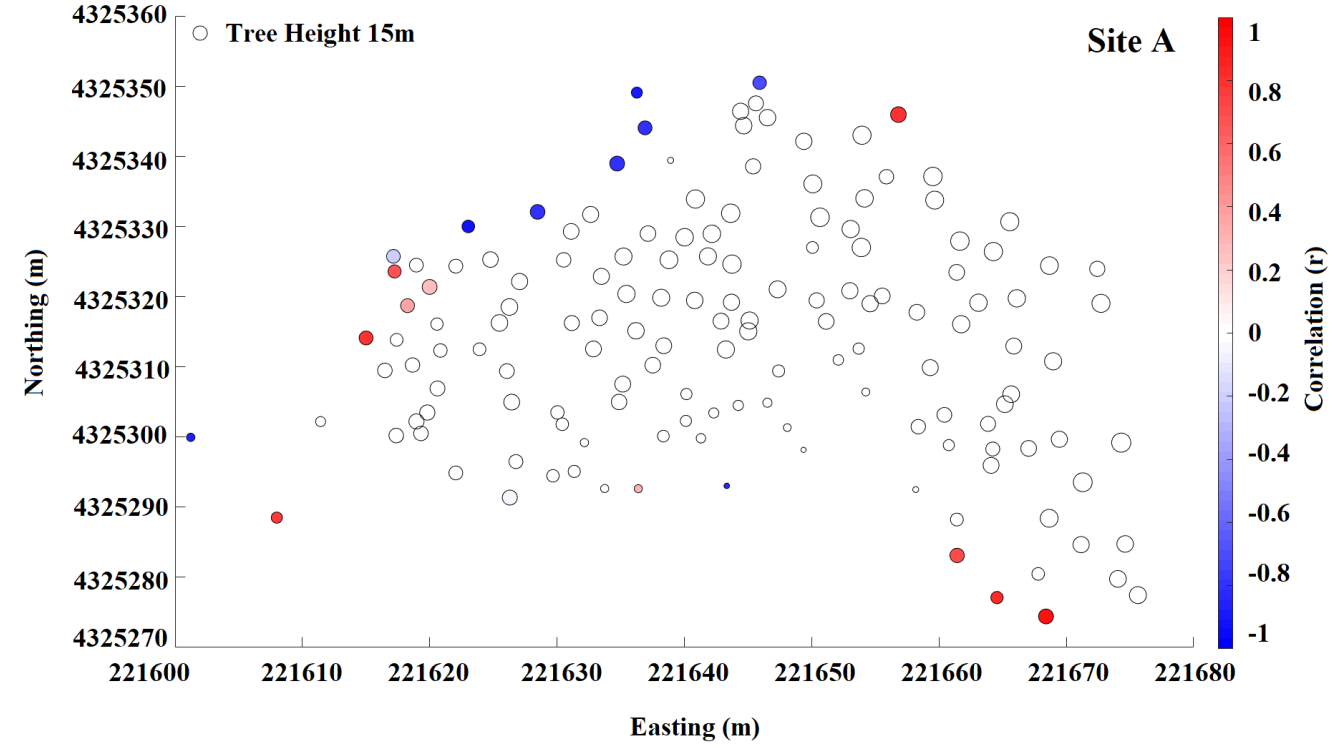

Figure B2: Correlation between distance from the edge of a tree and snow depth at site A. Correlations are shown for individual trees at each site with adequate snow coverage.

https://doi.org/10.5194/tc-2020-277
Preprint. Discussion started: 23 October 2020

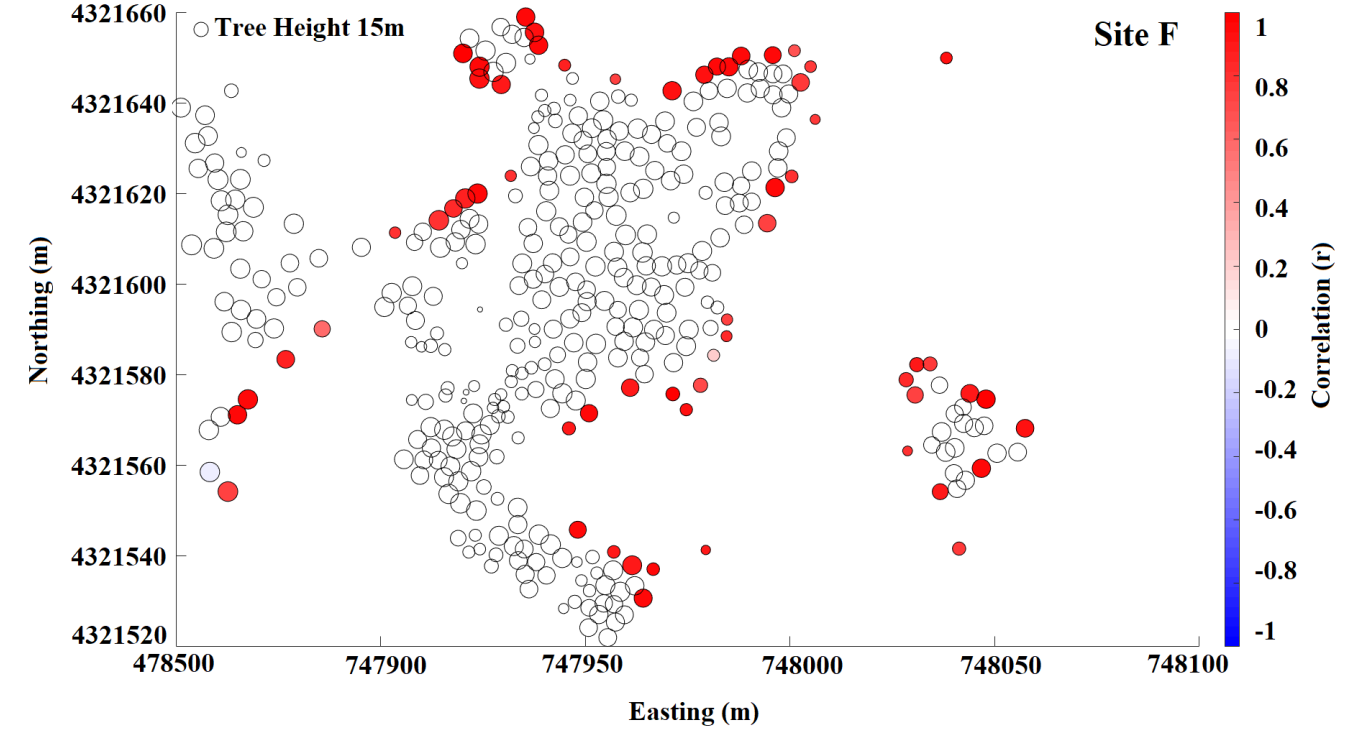

Figure B3: Correlation between distance from the edge of a tree and snow depth at site F. Correlations are shown for individual trees at each site with adequate snow coverage.

https://doi.org/10.5194/tc-2020-277
Preprint. Discussion started: 23 October 2020

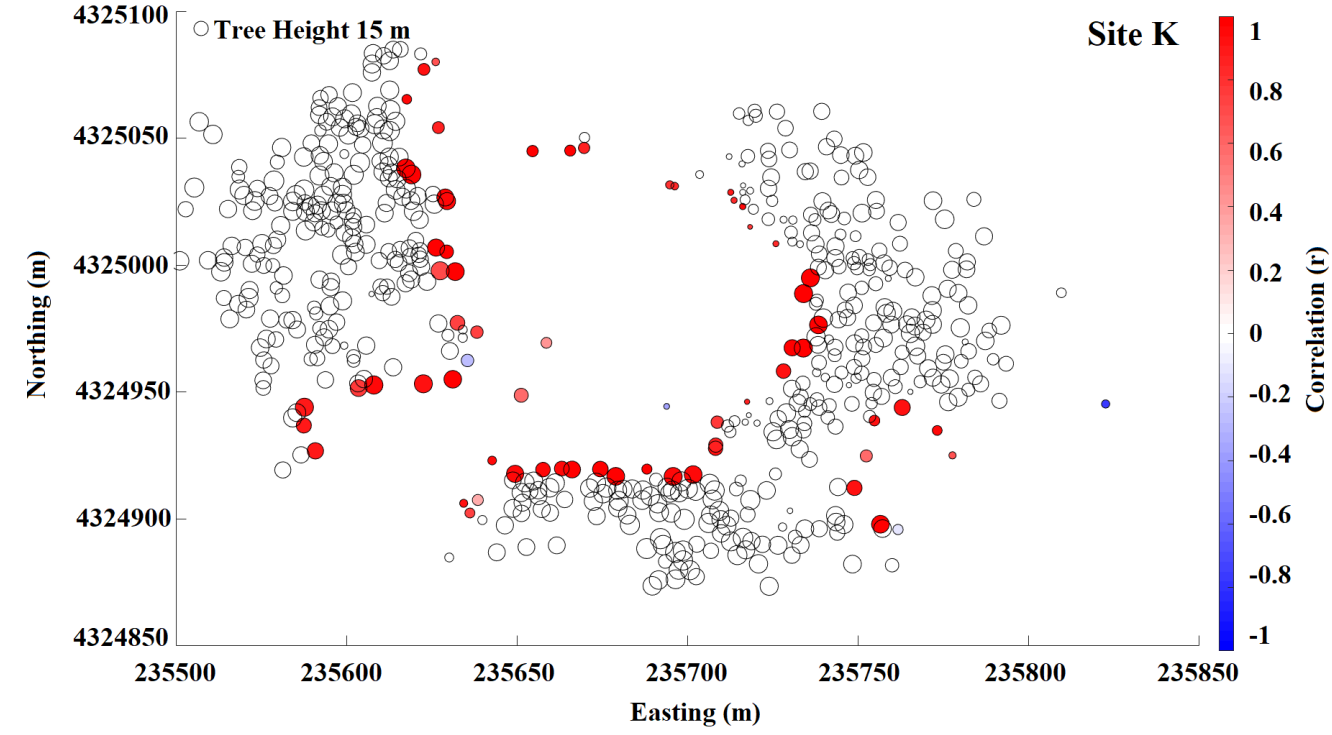

Figure B4: Correlation between distance from the edge of a tree and snow depth at site K. Correlations are shown for individual trees at each site with adequate snow coverage.

https://doi.org/10.5194/tc-2020-277
Preprint. Discussion started: 23 October 2020

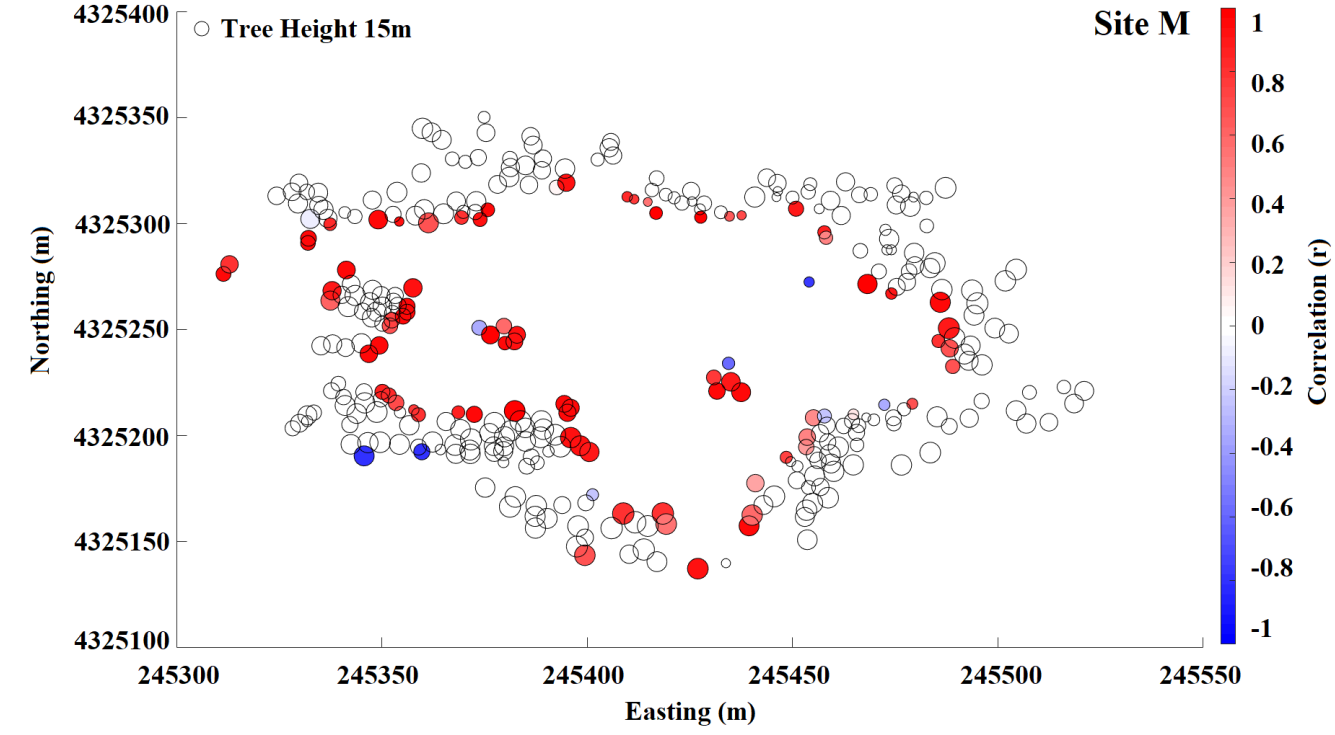

520 **Figure B5: Correlation between distance from the edge of a tree and snow depth at site M. Correlations are shown for individual trees at each site with adequate snow coverage.**

https://doi.org/10.5194/tc-2020-277
Preprint. Discussion started: 23 October 2020

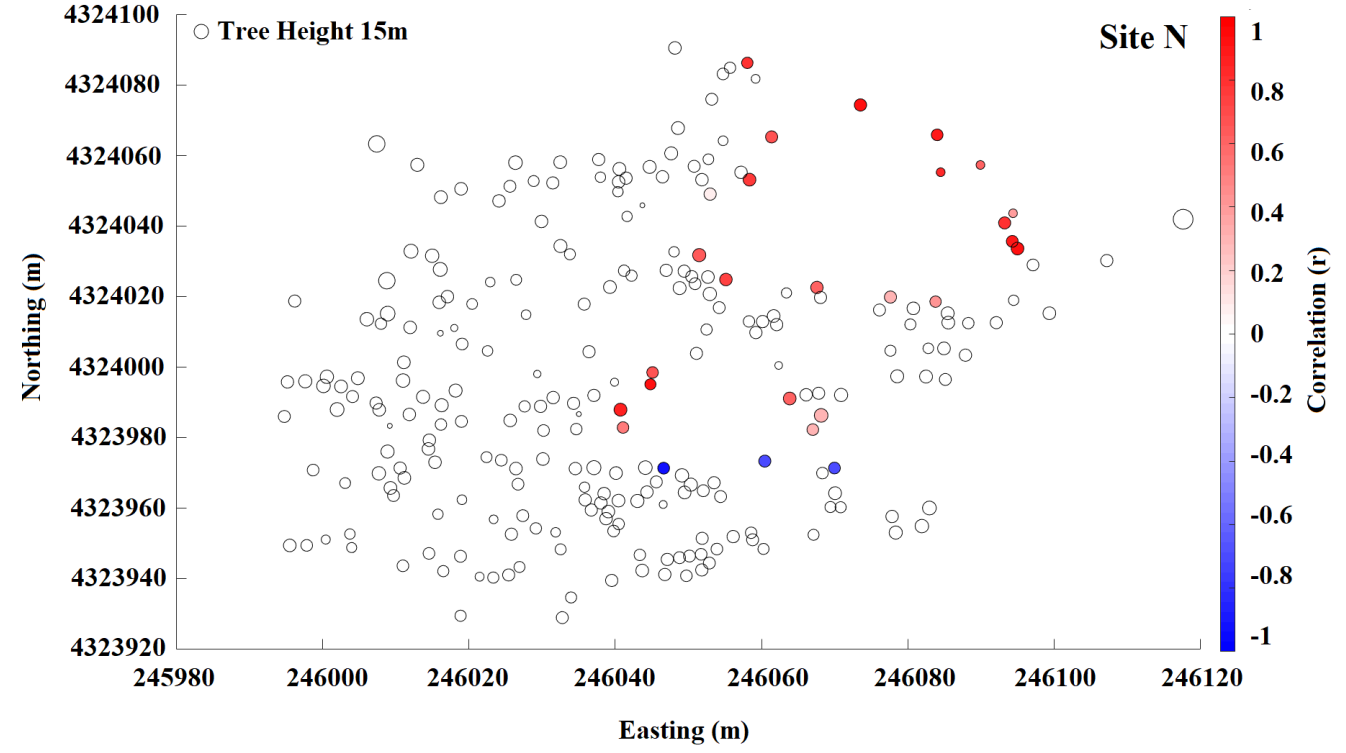

Figure B6: Correlation between distance from the edge of a tree and snow depth at site N. Correlations are shown for individual trees at each site with adequate snow coverage.

https://doi.org/10.5194/tc-2020-277
Preprint. Discussion started: 23 October 2020

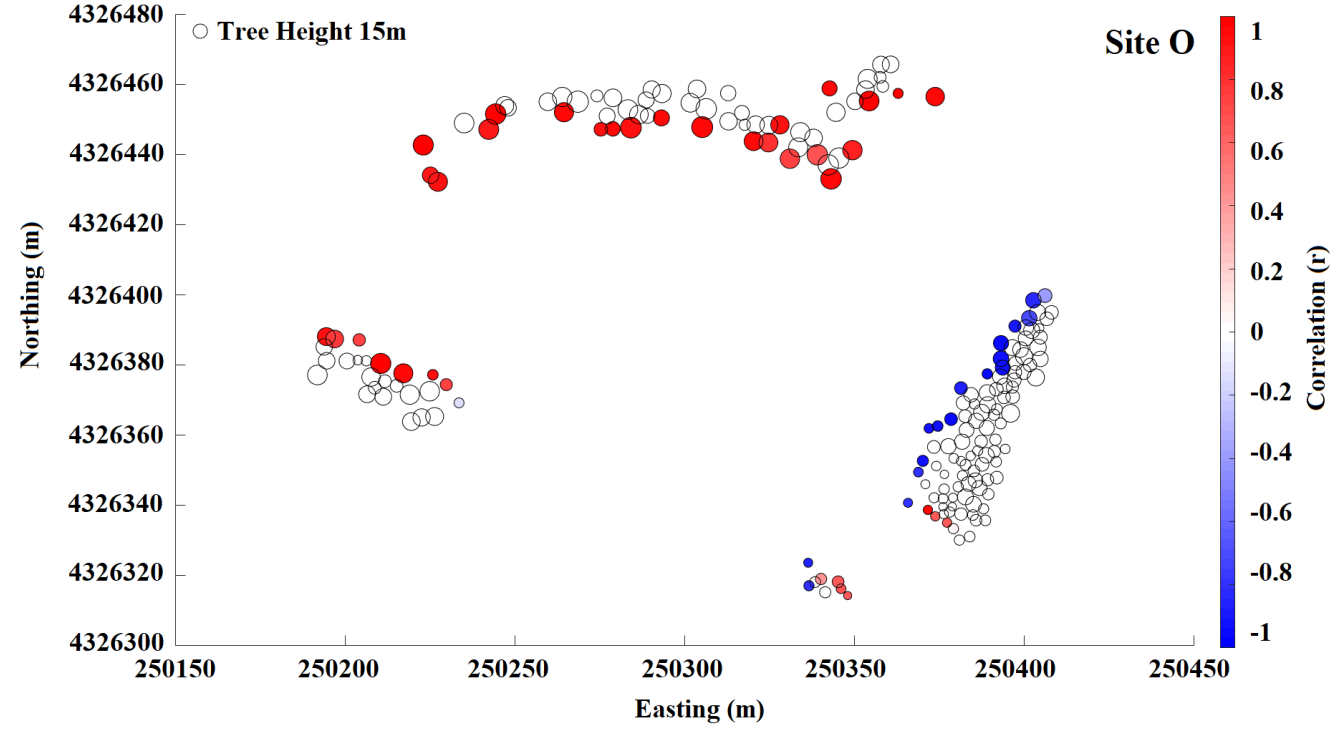

525

Figure B7: Correlation between distance from the edge of a tree and snow depth at site O. Correlations are shown for individual trees at each site with adequate snow coverage.

https://doi.org/10.5194/tc-2020-277
Preprint. Discussion started: 23 October 2020

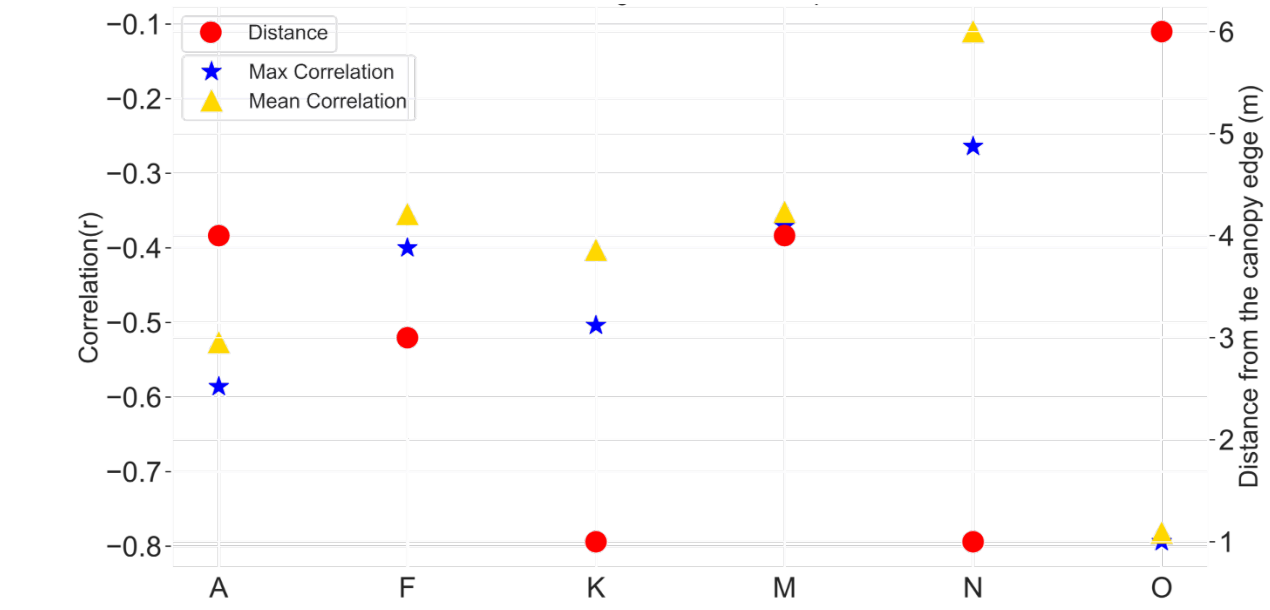

Figure B8: Correlation between maximum tree heights and snow depth with distance at each site. The maximum correlation (blue stars) corresponds to the distance marked with red (circles). This analysis was performed with 1 m bins of snow depth and all maximum tree heights at each site.

https://doi.org/10.5194/tc-2020-277
Preprint. Discussion started: 23 October 2020

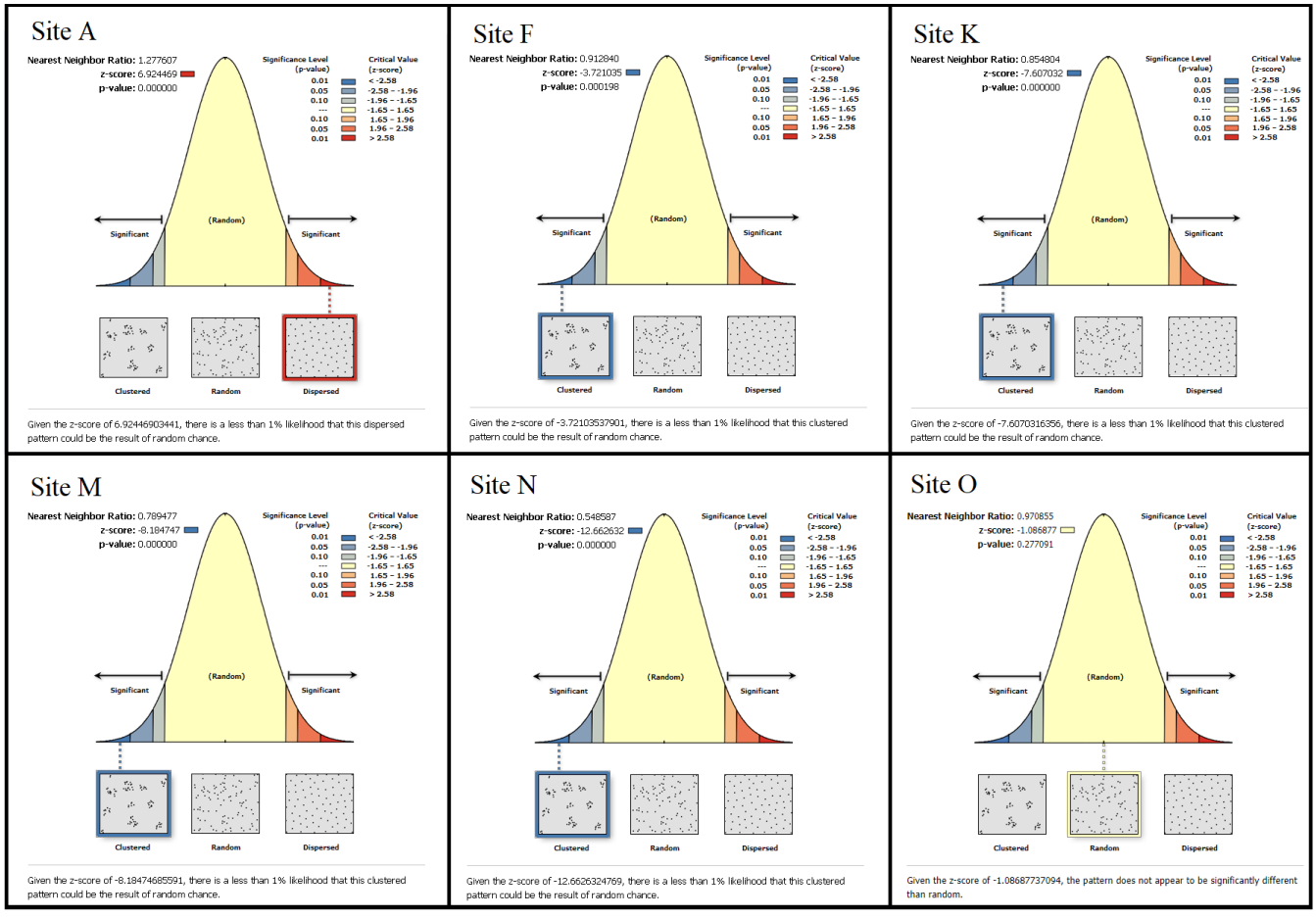

Figure B9: Average nearest neighbour results for each site. Only site N has a random distribution pattern of trees.